Part VI
Offshore Wind Farm Design

Chapter 19
An Overview of Offshore Wind Farm Design

Gregor Giebel and Charlotte Bay Hasager

Abstract For offshore wind energy to be viable, the design of wind turbines is not the only important factor—rather, the design of wind *farms* is also crucial. The current chapter discusses the challenges of designing an optimum wind farm and identifies the various factors that need to be considered. Lastly, the chapter presents the novel EERA-DTOC tool for designing offshore wind farm clusters.

19.1   An Overview of Offshore Wind Farm Design

There are two stages in the design of offshore wind farms, run by two different stakeholders. The first stage is often the choice of sites for tendering through a national authority, such as the Danish Energy Agency or the Crown Estate in the UK. During this stage, a number of different exclusion zones have to be managed, such as nature reserves, shipping lanes, oil exploration areas, light house cones, risks of unexploded ordnance or the chances for finding archaeological remains. Typically, the locations thus determined will be opened in a call for tenders, where the second stage of the wind farm design is done at the wind power developers. They now look into wind, wave and sea bed conditions, availability of foundation and turbine types and installation ships, layout of the wind farm, both taking wakes and cabling into account, projected operation and maintenance cost, and try to roll all of this information into typically a bid for a price per produced kWh. In some jurisdictions, the cost of transporting the power onshore is priced in with the wind farm, in other places the transmission system operator will have the duty of providing a suitable grid connection point in the vicinity of the wind farm. Usually, the cheapest bidder will be awarded the contract. Once that has happened, the detailed design of the wind farm will go on, including in-depth investigations of the sea bed, contracting of suppliers of hardware and services, detailed layouting of the farm, and finally the construction. As the last step before power delivery, the transmission system operator will check for grid code compliance, together with the checkout of the

G. Giebel (✉) • C.B. Hasager

Department of Wind Energy, Technical University of Denmark (DTU), DTU Risø Campus, Frederiksborgvej 399, 4000 Roskilde, Denmark
e-mail: grgi@dtu.dk; CBHA@dtu.dk

suppliers. Then, the wind farm will go into an operational state and will produce power for the next 25 years.

19.2 Strategic Planning

The first real offshore wind farm was built in Denmark, in 1991 in Vindeby. It consists of 9 Bonus 450 kW turbines on gravity foundations. It was followed by the similar sized wind farm at Tunø Knob in 1995. Both sites are in relatively protected Danish waters, and are now owned and operated by DONG Energy. Also for the permitting of the wind farm, the process was new and had to be a collaborative work of the Danish Energy Agency (DEA) as the permitting government authority and Elkraft, then the executing developer. A similar process still exists in Denmark under the name of Open-Door Policy, where new projects can be proposed and then will make their way through the permitting process. However, the more relevant process in recent years is the tendering process, where first parliament agrees on the size and overall location of the next Danish offshore farm, and then the DEA investigates the area and designs a call for tender. This was the procedure for the first large-scale offshore wind farm at Horns Rev in 2002, with 80 turbines and 160 MW total, and it has been refined ever since. The developer bids in with a price per kWh produced by the offshore wind farm. In this way it is hoped that the overall prices for offshore wind power come down over time.

Uncertainty about the input parameters for the wind farm design leads to higher prices from the developers. Therefore, already for the tender for the Anholt wind farm the Danish Climate and Energy Ministry changed the process so that the relevant sea bed investigations and the Environmental Impact Assessment (EIA) was handled and the outcome be known before the bids were given (Energinet.dk 2010). In this EIA, coordinated by the Danish Transmission System Operator Energinet.dk, a larger area was investigated in detail before the final call for tenders was published with regard to sea bed conditions, hydrography, geomorphology, coastal morphology, water quality, marine life and vegetation, benthic habitats, fish, birds, marine mammals, landscape issues, raw materials, marine archaeology, recreational areas, protected areas, ship and aerial traffic, fishery and others, during construction, operation and dismantling.

The influence of uncertainty on the price was exposed during the process leading to the Anholt wind farm. In this case, the Danish parliament required a new offshore wind farm to be built in too short a time to get a good process underway. This resulted in only one bidder (DONG Energy), who then claimed that the preparation time was too short to bring the uncertainties down, and added a significant mark-up to the best guess price. The next tender leading to the Horns Rev 3 wind farm had longer time for bidding, and subsequently for construction, and therefore attracted several bids. The outcome was 32 % cheaper than the price at Anholt. This price means, according to the Danish Ministry for Climate, Energy and Buildings, an economic benefit for rate payers in the order of 2.2 billion kroner over the lifetime

of the wind farm, in comparison to previous cost estimates (EFKM Denmark 2015). While this in part is due to moving technology (larger turbines were available since) and a better wind climate, reduced uncertainties also were a factor.

In the UK, the Crown Estate administers all the sea bed outside the 12-mile zone, and thus is the regulating authority for offshore wind farms in the UK. In three tendering rounds, the Crown Estate has increased the size of the area one could bid for, to the current Round 3 sites with over 1 GW potential each. Wind farms in the UK, despite an at least comparable wind resource to Denmark, are netting a higher strike price (in a "Contracts for Difference" scheme, the fixed price paid per kWh for the first e.g. 15 years; the premium is then the difference between the market price and the strike price) than their Danish counterparts. One important difference is that the transmission is in Denmark, but also in e.g. Germany, taken care of by the TSO. Thereby, the cost of transmission is spread over the total customer base of the TSO. In the UK, the transmission is a part of the strike price and therefore has to be financed as part of the wind farm investment.

19.3   Offshore Wind Farm Design

The main driver for wind farm design is the cost of energy. A simple model for the Levelised Cost of Energy, LCOE, is shown in Eq. (19.1):

$$LCOE = \frac{CaPEX \bullet CRF + OpEX}{AEP} \tag{19.1}$$

where CaPEX is the Capital Expenditure (i.e. the cost of wind turbines, foundations, cables, transmission system etc., their installation and financing), CRF is the Capital Recovery Factor (essentially a simplified representation of the discounted cash flow), OpEX are the Operating Expenses (i.e. operation and maintenance expenses), and AEP is the Annual Energy Production. Within this model, several sub-models are amenable to optimization. For example, in a radial cabling layout in the wind farm, where one radial connects a string of turbines to the substation, the cables further from the substation carry less electricity and could therefore be of smaller diameter. However, the installation cost can be double the cost per metre than the cable itself, and changing the cable on the installer ship incurs lost time too, so the optimization is less straightforward than just determining the electrical needs.

Construction of the offshore farm is a major cost factor. The industry has moved to dedicated ships installing the foundations and turbines, working as jack-up barges (Fig. 19.1) for a stable working platform in up to 30+ m water depth. Those ships can cost up to 200,000 €/day, and can install up to 2 turbines a day in optimal weather conditions. In larger wind farms, many processes work in parallel, installation of foundations, cable laying, removal of Unexploded Ordnance (UXO), diving for cable connection or inspection of the works done, and other things. For example, at the peak of construction of the currently largest offshore wind farm,

Fig. 19.1 A2SEAs SEA JACK during the construction of the Gwynt y Mor wind farm. Image Source: A2SEA (2016)

there were 1000 people working simultaneously on 60 vessels in the London Array (2016) site.

The OpEX is, to a large degree, determined by maintenance cost—both scheduled preventive and corrective maintenance, and the related lack of availability. The optimization of those depends heavily on the weather windows for accessibility of the farm. Already in 2001, Risø National Laboratory (now part of DTU) presented a tool to estimate weather windows and calculate the corresponding availability and outages of the turbines (Christensen and Giebel 2001). A main factor was the wave pattern at the site, as the significant wave height was more often a determining factor than too high winds. In 2012, researchers from University of Strathclyde (Dinwoodie et al. 2012) presented a similar picture using actual data: the availability in winter for three actual wind farms was significantly lower than in summer, which was attributed to the lack of accessibility to the sites (Fig. 19.2). In a notional 300 MW wind farm, this difference would mean over 2 million euros per month in lost production.

Finally, the last factor going into the determination of the LCOE is the AEP. Since usually, the wind distribution is mostly given by the choice of site by the national authority, and since the wind speed is not varying strongly across the area offshore (at least for current wind farm sizes sufficiently away from the shore), the most determining factor are the wake effects. By their very nature, wind turbines extract energy out of the wind, which means that the wind behind a turbine is less strong. If that diminished wind speed then comes to the next turbine, that turbine will produce less than if it was in free flow conditions. Researchers developed models to calculate this effect already in the 1980s, and by now a wealth of models with
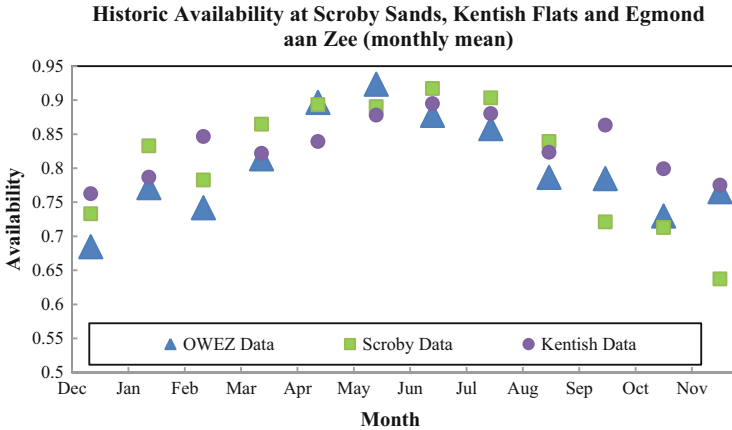
Historic Availability at Scroby Sands, Kentish Flats and Egmond aan Zee (monthly mean)

Fig. 19.2 Availability of three wind farms in the Netherlands and the UK. Source: Dinwoodie et al. (2012)
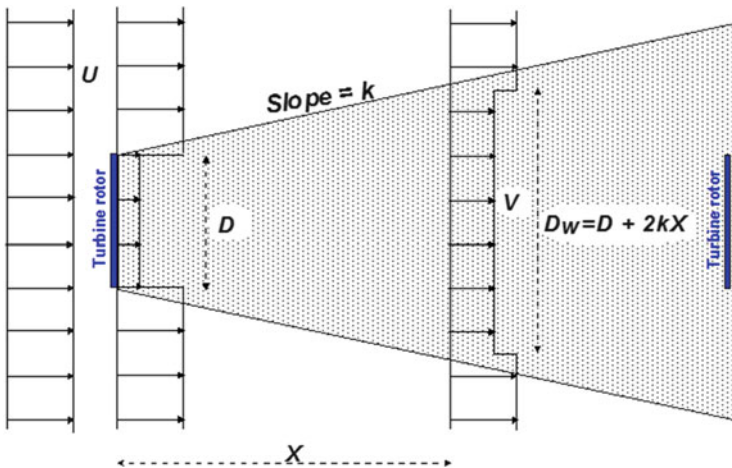

Fig. 19.3 Wake deficit and expansion as modelled by the PARK model of N.O. Jensen

varying degrees of sophistication have been developed. One of the simplest models is the PARK model developed by N.O. Jensen (Fig. 19.3), embodied in the siting software WAsP (2016). In reality, the wake expansion covers the fact that the wake expands relatively little, but meanders right and left in the atmospheric turbulence, which in the 10-min averages usually used for the AEP calculations gives the average wake loss given by the picture. Offshore, due to the reduced turbulence, the expansion parameter k is different from its onshore value. On the other end of the scale, Computational Fluid Mechanics (CFD) and Large Eddy Simulation (LES) models can calculate the wind flow in a wind farm with much higher resolution, but require significantly more running time, up to weeks on a supercomputer.
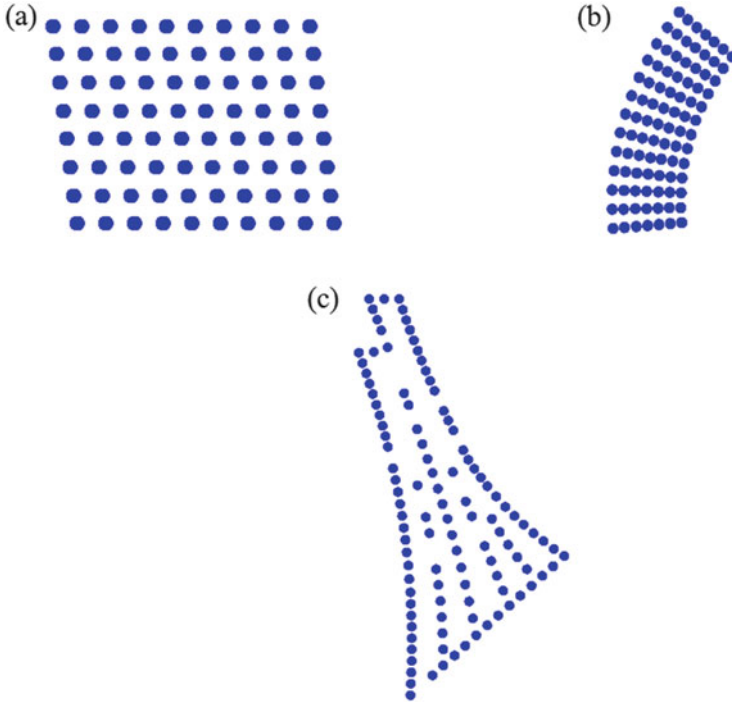
Fig. 19.4 The layouts of the (**a**) Horns Rev 1, (**b**) Horns Rev 2 & (**c**) Anholt OWFs. Source: Nygaard (2015)

Some major parameters with which to influence the total wake loss in a wind farm are the turbine spacing and layout. One can distinguish different generations of designs when looking at the development of the Danish offshore wind farms.

The first attempts were regular layouts like the one at Horns Rev 1 (and Nysted, built a year later), as shown in Fig. 19.4a. However, since the wake effects are very sensitive to the wind direction, already small changes in wind direction (as they happen frequently) will change the power output of the farm significantly, making the power less predictable and more difficult to integrate into the grid. This insight led to a second generation layout like the Horns Rev 2 (Fig. 19.4b), and Rødsand wind farms. Since the straight lines in the wind farm are not pointing into the same direction, the sensitivity towards wind direction changes is much reduced.

For the Anholt wind farm (Fig. 19.4c), built in 2012, developer DONG Energy chose a different layout. A more thorough assessment of the wake effects led to a perimeter centred layout, based on the notion that the second row shows the strongest wake effects, so an elimination of the second row will reduce the overall wake effects. However, this is not precedence for future wind farms. Also after Anholt there were farms planned in the UK with more regular layouts.

RS-2 20130430 17:41:53 UTC SAR intensity image
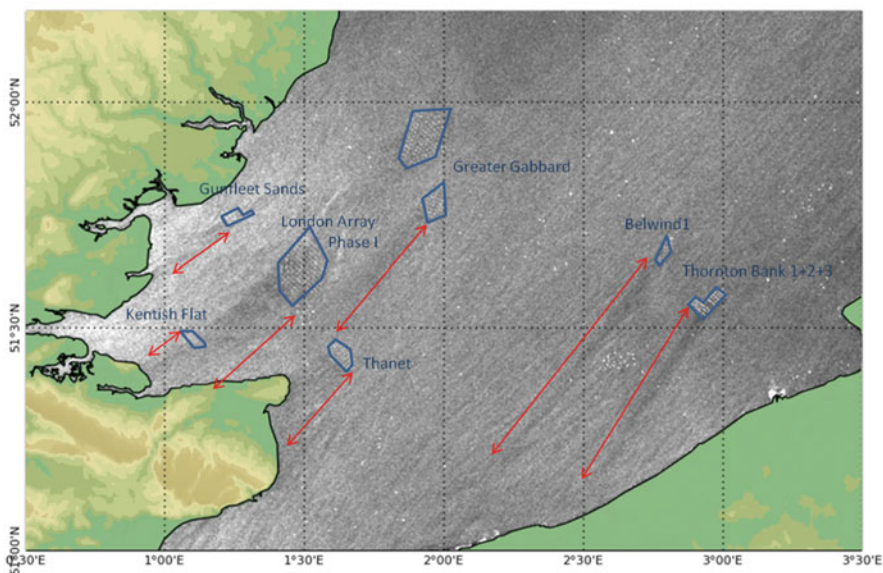
Fig. 19.5 RADARSAT-2 intensity map of the southern North Sea observed 30 April 2013 at 17:41 UTC. The *blue lines* outline wind farms and the *red arrows* the wind farm wake. The SAR-wind processing chain was set up by Collecte Localisation Satellites (CLS). Source: Hasager et al. (2015)

Wakes are not only an issue within a wind farm, they also extend for many km downstream of the wind farm. The wind speed near the sea surface can be measured using Synthetic Aperture Radar (SAR), e.g. mounted on satellites (Hasager et al. (2015)). In certain weather situations, the area of reduced production can extend several tens of kilometres. At Belwind wind farm the wake is around 55 km long, at Thornton Bank 45 km, at London Array 15 km, at Thanet 14 km and at Kentish Flat 10 km (but probably continues inland). It is the intensity image where the darker area is due to lower wind speed (Fig. 19.5).

19.4 EERA-DTOC and Wind & Economy

Over the last 3.5 years, the European Energy Research Alliance (EERA) integrated many of the institutes' softwares into a common Design Tool for Offshore Clusters (eera-dtoc.eu) in a project sponsored by the EU in years 2012–2015 (project budget 4 million euro). While strategic planners were envisaged as a potential target group, owing to the consortium membership in the EERA-DTOC project, the main emphasis went into making a good tool for offshore wind farm developers

(DTU Vindenergi 2016). Therefore, it integrated the workflow and the models from different planning aspects, i.e., wind climate, wakes and electrical models from grid to turbine plus a LCOE model, which currently embodies the cost function of an offshore developer. A number of EERA members' state-of-the-art models and software products, most notably DTU Wind Energy's own but also tools for the design of the grid inside the farm and the connection to the shore were integrated in the Design Tool for Offshore Clusters (DTOC) (Hasager and Giebel 2015). The tool, also commercially available under the name *Wind & Economy* (Wind and Economy 2016), was designed, integrated and developed by Overspeed, a SME from Oldenburg with specialty in wind consultancy and wind related software development.

The EERA-DTOC tool was designed based on input from end users. Its aim is to support the optimisation of LCOE by comparing different variants for the farm layout. A central concept of the DTOC tool is the organization of wind farm variants as scenarios and scenario trees. The single scenario is a fine-grained project variant, distinguished by all project parameters and the employed model chain including the model parameters. Scenarios can be cloned or duplicated, and inherit the settings from the higher level scenario.

This philosophy supports one of the central user stories (i.e., use cases): '*As a developer I can determine the optimum spacing, position, turbine model and hub height of turbines within an offshore wind farm*'.

The DTOC software supports the generation and comparison of the calculation results of many design scenarios. Comparative reporting of those results enables then the selection of optimized configurations. The work flow to optimize through comparing LCOE is shown in Fig. 19.6.

In order to calculate the LCOE, the submodels for e.g. cabling, AEP and grid compliance have to be called for each scenario. GIS data is also integrated in the tool, taking thus e.g. bathymetry into account. The runs start with the calculation of the wind climate calling a remote WRF installation at one of the three offering centres (DTU Wind Energy, CENER or CIEMAT). Typically, two or three runs are made, one run calculating a wind climate without any wind farms, one run with all currently running farms, and one run also including future wind farms planned in the
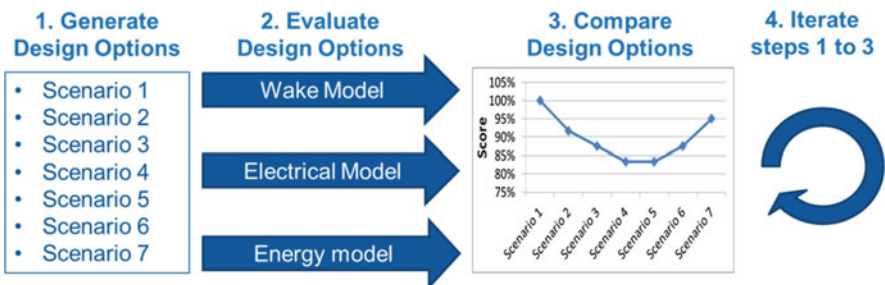

Fig. 19.6 Work flow for the DTOC-tool based optimization process

area. In this way, a timeline can be established when the production is going to drop due to wake effects from new wind farms. Since this wind climate is notionally the same for all wind farm configurations, it is run only once. This wind climate is then put into different farm layout options, which are compared according to Fig. 19.6. Therefore, instead of having to convert data from one program to the next, the user can handle many more scenarios before the bidding process begins.

References

A2SEA (2016) A2SEA Gwynt y Mor SEA-JACK. w.a2sea.com/wp-content/uploads/2014/07/A2SEA_Gwynt_y_Mor_SEA-JACK.jpg. Accessed 12 Apr 2016

Christensen P, Giebel G (2001) Availability of wind turbines in remote places. A statistical and a real-time view. Paper presented at the 2001 European wind energy conference and exhibition, Copenhagen, 2–6 July 2001

EFKM Denmark (2015) Danmark får billigere strøm fra havvindmøller. http://www.kebmin.dk/nyheder/danmark-faar-billigere-stroem-havvindmoeller. Accessed 12 Apr 2016

Dinwoodie I, Quail F, McMillan D (2012) Analysis of offshore wind turbine operation and maintenance using a novel time domain meteo-ocean modeling approach. Paper presented at the ASME Turbo Expo 2012: Turbine technical conference and exposition, Copenhagen, 11–15 June 2012

Energinet.dk (2010) Anholt Havmøllepark – Vurdering af virkninger på miljøet, VVM redegørelse. In: Energy Styrelsen Denmark files on renewable-energy, wind-power, offshore-wind-power and environmental-impacts. Available via ENS DK. http://www.ens.dk/sites/ens.dk/files/supply/renewable-energy/wind-power/offshore-wind-power/environmental-impacts/anholt_havmoellepark_vvm-redegoerelse.pdf. Accessed 12 Apr 2016

Hasager CB, Giebel G (eds) (2015) EERA-DTOC final summary report. In: European Energy Research Alliance – Design Tool for Offshore Wind Farm Cluster files (EERA-DTOC). Available via EERA-DTOC. http://www.eera-dtoc.eu/wp-content/uploads/files/D7-20-EERA-DTOC-final-summary-report-web-version.pdf. Accessed 12 Apr 2016

Hasager CB, Vincent P, Badger J et al (2015) Using satellite SAR to characterize the wind flow around offshore wind farms. Energies 8(6):5413–5439. doi:10.3390/en8065413

London Array (2016) Offshore construction. http://www.londonarray.com/the-project-3/offshore-construction/. Accessed 12 Apr 2016

Nygaard NG (2015) Wake model uncertainty quantification – a systematic approach. Paper presented at the EWEA offshore 2015 conference, Copenhagen, 10–12 Mar 2015

DTU Vindenergi (2016) Streamlining project planning of offshore wind farms. http://www.vindenergi.dtu.dk/Nyheder/Nyhed?id=C3435BFD-EF12-42CF-8F39-FD5FA8E948C8. Accessed 12 Apr 2016

WAsP (2016) WAsP website. www.wasp.dk. Accessed 12 Apr 2016

Wind And Economy (2016) Wind and economy. http://wind-and-economy.com/home/. Accessed 12 Apr 2016

Chapter 20
Large Eddy Simulation of Wind Farm Aerodynamics with Energy-Conserving Schemes

Dhruv Mehta

Abstract In order to truly realise the potential of wind power, it is vital to understand the aerodynamic losses over a wind farm. The current chapter highlights the importance of aerodynamic analysis of offshore wind farms, and presents a summarized review of Large Eddy Simulation literature. Furthermore, the chapter presents the objectives of the current research and concludes with a case study.

20.1 Introduction

This chapter presents a study on the Large Eddy Simulation of wind farm aerodynamics. Wind farm aerodynamics (WFA) deals with the interaction between wind turbine wakes and the atmospheric boundary layer (ABL), as they develop across the length of the wind farm. At times, the wakes also interact with each other and with other wind turbines (Mehta et al. 2014).

The study of WFA is crucial as it provides insight into the air flow through a wind farm, which eventually provides the energy that is converted into electricity by wind turbines. Therefore, one can assess the power produced by a wind farm by aerodynamically analysing the flow through the farm. The study of WFA requires aerodynamic data, which is generally gathered through meteorological masts in existing wind farms.

With the apparatus placed on these masts, we can measure the velocity and turbulence intensity (TI)—albeit at only a single point. In case the apparatus is an array of instruments, one may be able to measure the velocity (and TI) at more than a single point. Nonetheless, even in the best cases, the aerodynamic data for a few points on a wind farm is not enough to assess the power produced by the wind farm. Further, the erratic nature of the atmosphere makes it hard to relate the measured velocity (or TI) to its cause. For example, one cannot be certain whether

D. Mehta (✉)
Wind Energy Research Institute (DUWIND), Delft University, Kluyverweg 1, 2629 HS Delft, Netherlands

Energy Research Centre of the Netherlands (ECN), Westerduinweg 3, 1755 LE Petten, Netherlands
e-mail: d.mehta@tudelft.nl

the measured velocity (or TI) is from a single turbine's wake, or due to a sudden gust through the farm etc. Thus, for a complete insight, it is important to complement experimental data with numerical data from simulations.

20.2 Simulation

To simulate the flow through a wind farm, one must numerically resolve the various eddies within the air flow. These eddies represent the different scales of turbulence. For a high Reynolds number flow, these eddies can be of various sizes (Pope 2000). In case of a wind farm, this difference in eddy sizes can be between a few millimetres corresponding to boundary layer on a turbine's blade, and a kilometre corresponding to the height of the boundary layer. When the energy of these scales is plotted against their size, one obtains the energy spectrum as shown in Fig. 20.1.

The largest scales are the energy-containing integral range and the smallest ones are the dissipative, Kolmogorov scales (Tennekes and Lumley 1972). In between lies the inertial range. On a wind farm, these scales are about a few centimetres in size.

It is computationally impossible (with today's resources) to resolve all these scales feasibly. Therefore, the wisest approach would be to numerically resolve only the large energy containing scales (and a part of inertial range), to gain insight into WFA. This approach is known as Large Eddy Simulation (LES); an example of
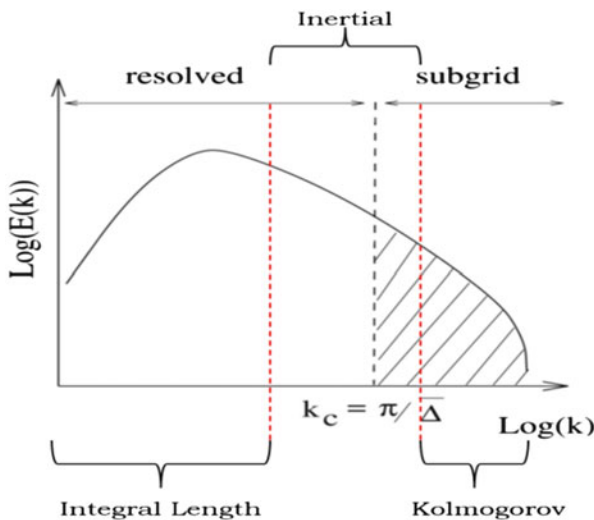
Fig. 20.1 The energy of the various eddies (y-axis) in a flow, plotted against their size (x-axis)
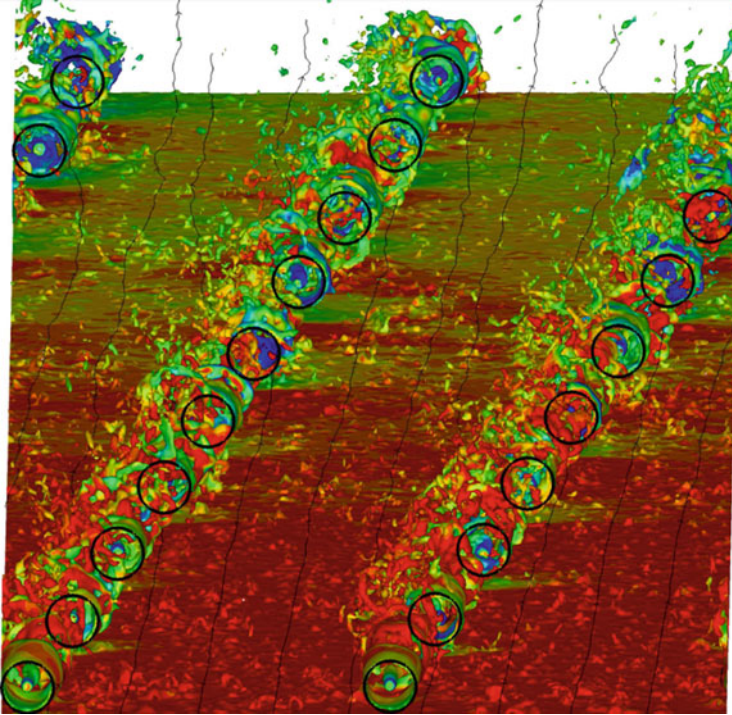
Fig. 20.2 Large Eddy Simulation of the Horns Rev wind farm [Source: Ivanell (2009)]

LES is shown in Fig. 20.2. As shown in Fig. 20.1, the scales that are numerically calculated are called the 'resolved scales' and the rest are known as the 'subgrid scales'. The latter are numerically modelled with a subgrid scale (SGS) model.

20.3   Literature Review

A comprehensive literature review on LES was conducted by Mehta et al. (2014). We summarize the key points below:

- Wind farms simulations have been performed predominantly with eddy-viscosity models. Even the simple Smagorinsky's model is sufficient for qualitative analyses of wind farm aerodynamics. But for accuracy, researchers must rely on more advanced SGS models.
- With proper ABL modelling, LES can help assess the performance of wind farms in off-design conditions like non-neutral ABLs and gusts. Effective coupling with aeroelastic codes could provide great insight into turbine loading in such situations.

- Wind farm simulations rely on accurate wake-ABL interaction, which is possible only with a correct ABL model. This is of great consequence for simulating large wind farms on which the ABL evolves into a wind turbine-ABL. Generating a synthetic ABL requires lesser computational effort than precursor simulations with LES, but lacks the statistical correlations that exist in a physical ABL.
- Using the Scale Dependent Dynamic model with Lagrangian averaging generates an ABL that is accurate enough for wind farm simulations, but is computationally expensive. Nonetheless, it retains its precision even on coarse grids making it suitable for LES.
- From simulations of the Horns Rev wind farm, it is apparent that the performance of engineering models is comparable to that of certain LES codes, as far as generating averaged statistics. When done with accurate ABL modelling and with advanced SGS models, on relatively refined grids, LES delivers a substantially better performance.
- LES data can be utilised to enhance simple engineering models to retain computational efficiency but ensuring better accuracy.
- Numerical schemes for LES must ensure zero numerical dissipation for high accuracy. Pseudo-spectral and Energy-Conserving spatial discretisation schemes are useful in this regard; the latter however requires a higher-order formulation to be as accurate as the former. Additionally, energy-conserving time integration with zero dissipation would help speed up computations, but requires further modifications to avert loss in accuracy and stability.
- A stress-free upper boundary is most appropriate for wind farm simulations. Periodic boundaries required by spectral schemes can be avoided with Energy-Conserving schemes, which are however not as accurate as the former.
- SGS models have been compared in terms of their ability to simulate the ABL. It is clear that above beyond a certain resolution, the effect of the SGS model on ABL is nullified and even a simple model is sufficient for an ABL simulation. However, such a conclusion with regard to wind farm simulations is yet to be drawn.

Concerning LES, it is certain that no SGS model is complete and their efficacy is situation-dependent. Smagorinsky's model and its derivatives are popular as they are easily implementable and capable of producing good data on wind farm aerodynamics, despite their assumptions lacking conclusive evidence. Regarding coarse grids, it would be wise to develop numerical schemes instead of relying on excess computational power. LES codes cannot count on upwind schemes of stability because the numerical dissipation will dampen the resolved scales, more so on coarse grids. High-order spectral methods are thus common in LES but are computationally expensive. On the other hand, Energy-conserving schemes are free from numerical dissipation and permit the use of non-periodic boundaries, but require further investigation at this stage.

In terms of boundary conditions, Monin-Obukov's (Panofsky and Dutton 1984) approach remains the only option for modelling the ABL, despite being deemed unsuitable for LES. Lately, research has been focussed on developing a more appropriate technique that could be adapted for inhomogeneous terrains, but experiments would be more instrumental in enhancing the existing approach.

20.4   Power Losses and Observations

Figure 20.3 shows the power generated by the various rows of wind turbines simulated as shown in Fig. 20.2. It can be observed that the power generation is the highest for turbines in the front row, which is exposed directly to the freestream ABL flow. However, turbines within this row generate a wake, which develops with downstream distance and interacts, in the case of Horns Rev, within downstream turbines.

Therefore, there is a sudden decrease in power generation by the second row. This is due to the reduced velocity in the wake. However, a wake not only bears a reduced velocity but also a higher turbulence intensity. This fact has been confirmed experimentally by Chamorro and Porté-Agel (2011) and numerically through LES by Stevens et al. (2013).

This increased turbulence promotes the mixing of the slower wake with the faster freestream ABL flow, leading to the reduction of the velocity deficit in the wake and increased velocity. This is the reason why the second row (Horns Rev,
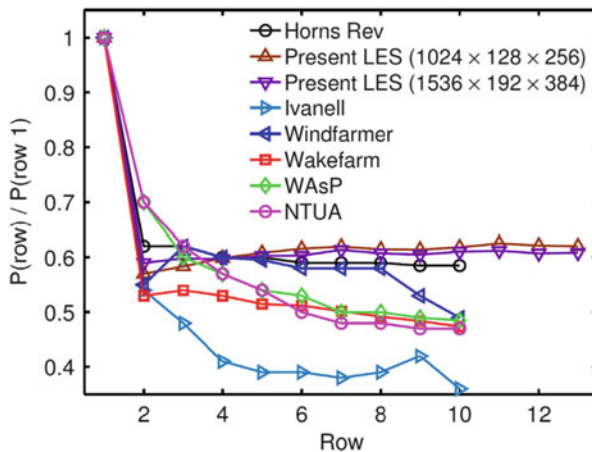
Fig. 20.3 The power output on the Horns-Rev wind farm predicted by an LES codes (present LES, and Ivanell (2009)) and various engineering models, adapted from Stevens et al. (2013). The power output on the y-axis has been normalised by the power output of the turbines in the first row. One notices the discrepancy between LES and simple engineering models

black line in Fig. 20.3), generates the highest power amongst all downstream rows. Further, the increased turbulence reaches a peak value after the wake from the first turbine interacts with the second turbine, leading to a slower wake; thus, after one wake-turbine interaction. At times, this could happen after two such wake-turbine interactions, in case the inflow turbulence is low (Mehta et al. 2014).

Once, the wake generated turbulence reaches its peak value, the recovery of the reduced velocity in the wake also reaches its limit. Therefore, after one or two wake-turbine interactions, the wake does not recover much, as a result, one notices a decline in power production across the rows on a wind farm. Nevertheless, the decrease is not steep as compared to the one noticed within the first two rows. The fact that the added turbulence has reached a steady peak value, ensures that the wake recovers after every wake-turbine interaction, to a value that is more or less similar to the inflow value. In effect, beyond the second or third row, the horizontal flow is fully developed, leading a similar power prediction as seen in Fig. 20.3 (Calaf et al. 2010).

Figure 20.3 also compares the date from LES and engineering models. These models are very simple and built upon the simplification of the flow phenomena. As a result, these models are fast and computationally efficient but not very accurate. Further, their accuracy is mostly related to the prediction of the average power output over a range of wind directions, and not for a particular inflow direction, which requires the application of LES (Barthelmie et al. 2009).

20.5   Research Objectives

The current research involves three phases:

- Implementing an SGS model in the Energy-Conserving Navier-Stokes (ECNS) code.
- Analysing energy-conserving (EC) spatial discretisation and EC time integration in terms of accuracy and efficiency.
- Validating the combination of the ECNS and the chosen SGS model for wind farm simulations.

20.6   Tests and Results

The following are the tests conducted, the results obtained and the conclusions drawn.

20.6.1 EC Time Integration

EC time integration available within the ECNS code is unconditionally stable for any time step. Further, it introduces no numerical dissipation during the simulation (Sanderse 2013). However, according to the literature, most existing LES codes would rely on non-EC time integration.

We therefore, used the case of decaying isotropic homogeneous turbulence, to assess whether an EC time integration scheme offers any advantage, in terms of accuracy. We observed that an implicit EC time scheme (4th order accurate), has a lower global error than a 4th order accurate, non-EC explicit time scheme. This error corresponds directly to the numerical dissipation (Fig. 20.4).

However, as shown in Fig. 20.4, the computational time required by the implicit EC time schemes, are much larger than those required by the explicit non-EC schemes. This disproportionality is such that, one is better off using a non-EC explicit time integration scheme (as done by existing LES codes) with a smaller time step, as opposed to an implicit EC scheme.
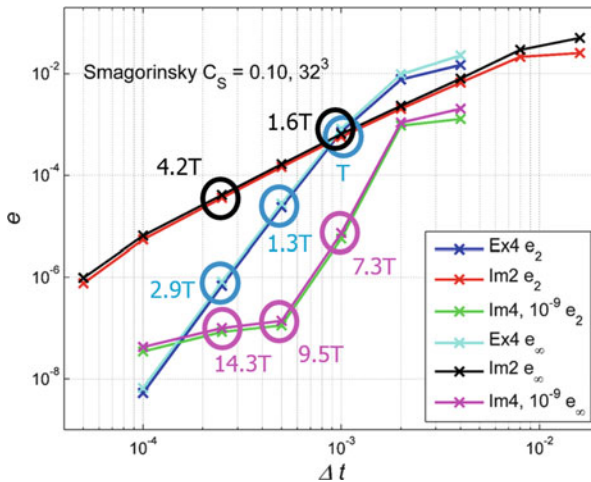
Fig. 20.4 A plot of the error vs. the time step use with three time integration methods: Ex4, explicit 4th order non-EC Runge-Kutta scheme; Im2, implicit 2nd order EC Gauss scheme and Im4, implicit 4th order EC Gauss scheme. T is the computational time take by Ex4 at a time step of 0.001 s

20.6.2   EC Spatial Discretisation

EC spatial discretisation done on a Cartesian staggered grid, is dissipation free for any grid size (Sanderse 2013). However, the scheme itself, is essentially a simple central difference scheme (Perić and Ferziger 2002).

We checked if using an EC spatial discretisation on a Cartesian staggered grid, is the same as using a simple central difference on a collocated Cartesian grid. Using a series of tests on inviscid vortices, we noticed that both the schemes are numerically alike. By extension, the absence of numerical dissipation in either scheme, reduces the grid dependence in tuning the Smagorinsky SGS model chosen for the ECNS (Fig. 20.5).

Therefore, we were able to tune the Smagorinsky model in the ECNS, to a value of the Smagorinsky constant, $C_S = 0.12$. Over a range of grid resolutions, this value of the Smagorinsky constant was reasonable enough to predict the behaviour of the large energy-containing scales, correctly.
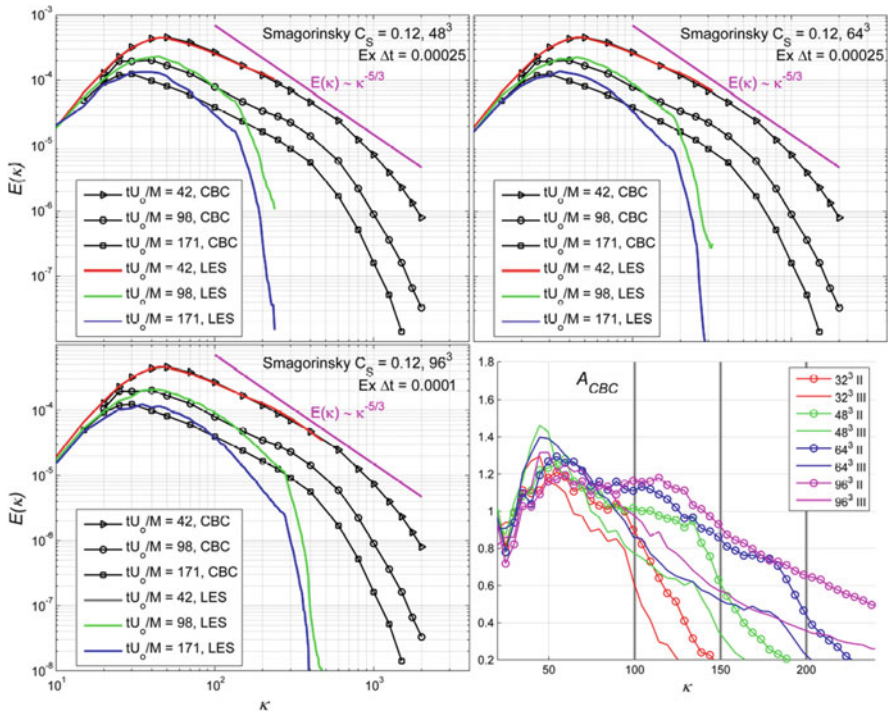
Fig. 20.5 Clockwise from *top-left*: the energy spectra obtained through experiments (Comté-Bellot and Corrsin 1971) compared against results with the ECNS and a Smagorisnky constant of 0.12, and three different grid resolutions. *Bottom-left*: the ratio of the simulated value of the energy at a given wavenumber to the experimentally obtained value at the same wavenumber
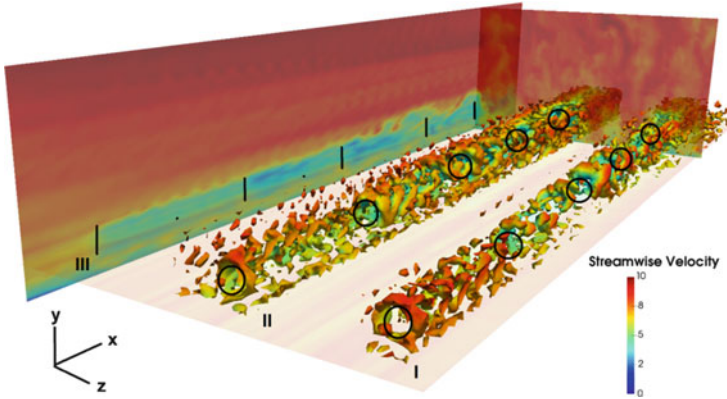
Fig. 20.6 Isosurfaces of Q-Criterion coloured by streamwise velocity in the wake of turbines on a simple wind farm. The ABL is neutral and runs through a wind farm with 15 turbines

20.6.3   Validation

The code with the chosen value of the Smagorinsky constant was validated against two test-cases.

- The simulation of an actuator disk's wave validated against particle image velocimetry measurements in the wake of a porous disc within in a wind tunnel, designed to emulate the actuator disk concept (Lignarolo et al. 2014).
- The simulation of a neutral-ABL with the ECNS-Smagorinsky model, to obtain the correct velocity profile and turbulence statistics (Meyers 2011).

The value of the Smagorinsky constant is fit for either case; as a result, we are able to simulate the combination of the actuator disk method and the neutral atmospheric boundary layer (Fig. 20.6).

20.7   Case Study: EWTW

We use the validated ECNS-Smagorinsky LES code to simulate the turbines at the ECN Wind Turbine Test-Site Wieringermeer (EWTW) (Bot 2015). It has five turbines of diameter $D = 80$ m, separated in the streamwise direction by 305 m or 3.812D. We simulate the turbines with an inflow velocity of 8 m s^{-1} at hub-height
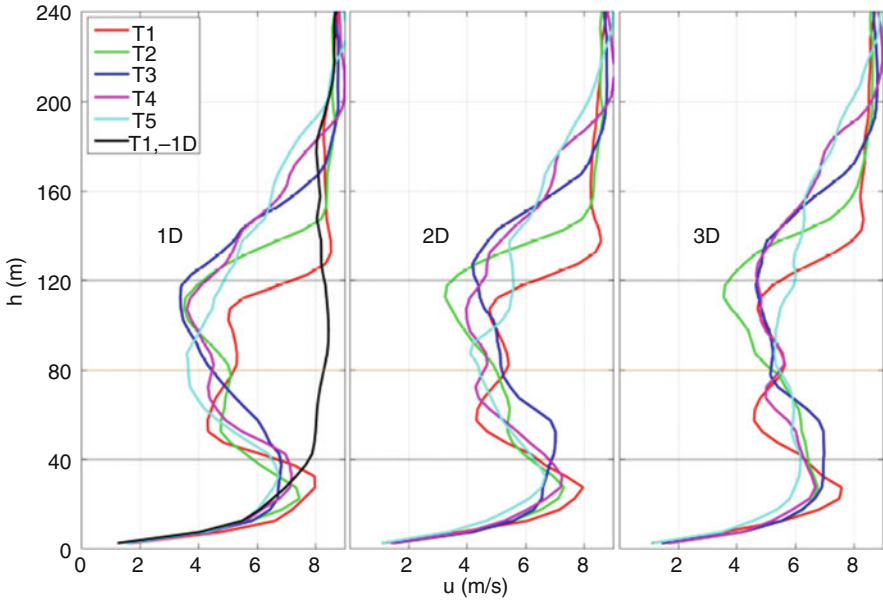
Fig. 20.7 Profiles of streamwise wake velocity behind the turbines at the EWTW

and a thrust coefficient of 0.789. We do not have ample experimental data to validate the ECNS, however, we do notice trends in the prediction of the wake velocity and turbulence intensity that are relevant to wake-turbine interaction across a row of turbines.

Figures 20.7 and 20.8 show the variation in velocity and turbulence intensity, respectively, with the vertical distance from the ground, behind 5 turbines, T1 to T5, at three downstream distances, 1D, 2D and 3D. In the leftmost plot within Figs. 20.7 and 20.8, the inflow profile has also been plotted (in black) at 1D before the first turbine, T1, or -1D. One notices trends similar to those explained in Sect. 20.4, regarding the recovery of velocity deficit, which is maximum behind the first turbine. However, the velocity recovers more rapidly behind the downstream turbines, as the turbulence intensity develops and reaches a fixed value, which aids the recovery of wake velocity.
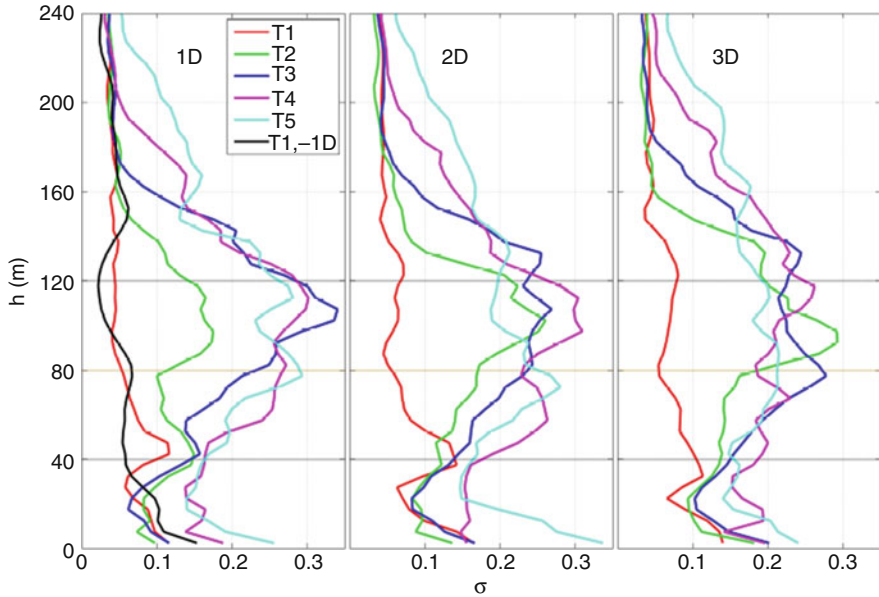
Fig. 20.8 Profiles of turbulence intensity behind the turbines at the EWTW

20.8   Conclusions and Recommendations

Based on the research we conclude the following:

- EC time integration is beneficial for averting numerical dissipation, which can lead the spurious decay of energy during wind farm simulations, and eventually, producing a wrong estimate of power generation. However, a non-EC time integration scheme can also guarantee minimal numerical dissipation at a small time step, at significantly lower computational costs.
- EC spatial discretisation helps tune the Smagorinsky model for a range of grid resolutions owing to the absence of numerical dissipation, which varies with grid resolution and must be accounted for while tuning.
- The Smagorinsky constant obtained through tuning the model for decaying isotropic homogeneous turbulence, can be used to simulate a neutral-ABL and the wake of an actuator disk and therefore, by extension, the flow through a wind farm.

For research in the future, we recommend the following:

- Developing an optimised method to using the EC time integration schemes more efficiently. Although non-EC schemes are a fine alternative, they are restricted by a stability criterion that prevents the use of local grid refinement. Such, refinement can help gain insight into critical phenomena in the wake and the

ABL as a whole. Using an EC time scheme that is implicit, will not only remove the restriction on grid refinement but also avert numerical dissipation.

- Simple schemes such as the central difference scheme in OpenFOAM can readily be used for wind farm aerodynamics, instead of developing new computational methods.

References

Barthelmie RJ, Frandsen ST, Hansen K et al (2009) Modelling the impact of Wakes on Power Output at Nysted and Horns. Paper presented at the EWEC 2009, European wind energy conference and exhibition, Marseille 16–19 March 2009

Bot ETG (2015) FarmFlow validation against full scale wind farms, Technical Report ECN-E-15-045. In: Energy research Centre of the Netherlands publications. Available via ECN. https://www.ecn.nl/publications/PdfFetch.aspx?nr=ECN-E--15-045. Accessed 12 Apr 2016

Calaf M, Meneveau C, Meyers J (2010) Large Eddy Simulation study of fully developed wind-turbine array boundary layers. Phys Fluids. doi:10.1063/1.3291077

Chamorro LP, Porté-Agel F (2011) Turbulent flow inside and above a wind farm: a wind tunnel study. Energies 4:1916–1936

Comté-Bellot G, Corrsin S (1971) Simple Eulerian time correlation of full and narrow band velocity signals in grid generated isotropic turbulence. J Fluid Mech 48:272–337

Ivanell SSA (2009) Numerical computations of wind turbine wakes. In: Technical reports from the Royal Institute of Technology, Linné Flow Centre, Department of Mechanics, Stockholm. Available via KTH. https://sverigesradio.se/diverse/appdata/isidor/files/3345/10845.pdf. Accessed 12 Apr 2016

Lignarolo L, Ragni D, Krishnaswami C et al (2014) Experimental analysis of a horizontal axis wind-turbine model. Renew Energ 70:31–46

Mehta D, van Zuijlen AH, Koren B et al (2014) LES of wind farm aerodynamics: a review. J Wind Eng Ind Aerod 133:1–17

Meyers J (2011) Error-landscape assessment of large-eddy simulations: a review of the methodology. J Sci Comput 49:65–77

Panofsky H, Dutton J (1984) Atmospheric turbulence: models and methods for engineering applications. Wiley, New York

Perić M, Ferziger J (2002) Computational methods for fluid dynamics. Springer, Berlin

Pope SB (2000) Turbulent flows. Cambridge University Press, Cambridge

Sanderse B (2013) Energy conserving discretisation methods for the incompressible Navier-Stokes equations: application to the simulation of wind-turbine wakes. Dissertation, Eindhoven University of Technology

Stevens RJAM, Gayme DF, Meneveau C (2013) Effect of turbine alignment on the average power output of wind farm. In: Abstracts of the ICOWES 2013 international conference on aerodynamics of offshore wind energy systems and wakes, Lyngby, 17–19 June 2013

Tennekes H, Lumley JL (1972) A first course in turbulence. MIT Press, London

Chapter 21
A Theoretical Risk Management Framework for Vessels Operating Near Offshore Wind Farms

Raza Ali Mehdi and Jens-Uwe Schröder-Hinrichs

Abstract The design of an offshore wind farm (OWF) can have a major impact on the safety of maritime operations in the vicinity. Factors such as the number of turbines, turbine spacing, and tower design can all have an effect the probability and consequences of various maritime accidents. The current chapter describes the potential effects of offshore wind farms on maritime traffic—particularly in a safety, reliability and risk context. The chapter also reviews existing methods, models and frameworks that can be used to assess the risk to maritime operations. Lastly, the authors propose an improved theoretical risk management framework that addresses some present concerns.

21.1 The Need for Maritime Risk Management Around Offshore Wind Farms

In this first section, the status of the OWF industry and the need for maritime risk management around wind farms is described.

21.1.1 Trends in the OWF Industry

Over the past few decades, there has been a sharp increase in the use of renewable energy—driven not only by a more mindful society, but also by strong policy instruments and decisions. One of the most popular renewable energy schemes is wind energy. As the demand for energy generation grows, an increasing number of wind turbines are being installed offshore. OWFs offer several advantages over their onshore equivalents. There is better wind resource, and the wind speeds are more consistent out at sea. Potentially, wind turbines can also be scaled up to much

R.A. Mehdi (✉) • J.-U. Schröder-Hinrichs
Maritime Risk and System Safety (MaRiSa) Research Group, World Maritime University, Fiskehamnsgatan 1, 21118 Malmö, Sweden
e-mail: rm@wmu.se; jush@wmu.se

greater sizes than would be possible onshore—leading to increased, more efficient, energy generation. In Europe, on average, an offshore wind turbine has a capacity of 3.6 MW and generates 12,961 MWh of energy annually; by comparison an onshore turbine has an average capacity of 2.2 MW, and generates around 4702 MWh of energy (EWEA 2015).

OWFs can also be constructed close enough to heavily populated shores to reduce energy transport cost, and yet be distant enough not to cause visual and noise pollution (Anderson 2013). These factors, combined—to some extent—with limited space on land, have led to an increased exploitation of marine areas for wind energy generation. As a result, offshore wind turbines are increasingly rapidly in size and numbers. Wind farms are also getting larger and moving further ashore so as to better exploit wind resource.

There are, however, certain drawbacks of OWFs that also need to be taken into account. The drawbacks include harsh environmental conditions for construction and maintenance, limitations in deep water installation technology, and impacts on the marine environment (Anderson 2013). These disadvantages, coupled with the high cost of capital investment, maintenance and reliability mean that OWFs are not as cost-effective or efficient as their onshore equivalents today; in fact, by certain estimates, the costs of operation and maintenance (O&M) for OWFs may be 2–6 times higher than those for onshore wind (Dalgic et al. 2013).

21.1.2 The Need for Maritime Risk Assessment and Management

Building an OWF has an impact on vessel operations in the vicinity. A wind farm leads to more obstructions in the water for ships to avoid; the presence of a wind farm near a shipping lane effectively narrows the area in which vessels can operate, therefore increasing the traffic density. This may lead to additional costs for the maritime industry—if for example, the vessels have to be diverted to sail along a longer route.

Perhaps more importantly, there is also an increased risk of accidents due to the increased maritime traffic as a result of activities related to OWFs. In addition to the increased traffic density, and reduced sea space, wind turbines may also cause problems with a ship's on-board navigation equipment. In fact, the potential accidents that maritime operations face due to offshore wind farms can be classified into five different categories.

- Navigational accidents involving passing vessels (Powered and Drifting)
- Navigational accidents involving wind farm support vessels
- Accidents during OWF installation and decommissioning operations
- Accidents during emergency maritime operations such as SAR
- Accidents in harbours and ports that deal with offshore activities

In addition to the risk-areas mentioned above, an OWF may also affect the safety of pleasure vessels and fishing operations; these areas, however, are beyond the scope of the current research.

Any of the maritime accidents listed above, if they occur in the vicinity of an OWF, may cause a farm-wide shutdown, or lead to a severe delay in installation, repair or maintenance services—thus leading to higher costs. In the worst case scenarios, maritime accidents may not only damage the vessels, but also the turbines—leading to further downtime and increased repair costs, thereby reducing the reliability of offshore wind even further. According to the findings of Dai et al. (2013), a fairly small support vessel with 230 tones displacement, colliding head-on with the landing structure on a turbine tower at a speed of just 0.48 m/s, would be enough to induce local yield in the structure; colliding a speed of 0.84 m/s with the landing structure would induce global yield. Conversely, the same vessel colliding head-on directly with the tower would cause local yield and global yield at speeds of 0.34 m/s and 0.55 m/s respectively. Such reports clearly highlight the need for thorough risk management.

Risk management may also be a legal or regulatory necessity—national, and international standards, e.g. BSH (2015) and MCA (2013), may require wind farm owners to demonstrate that their OWF will not impede the safety of maritime operations. In Germany, for instance, there are very clear guidelines which state that accidents near OWFs should not happen more than once every 100 years. Wind turbines installed in Germany must also be *collision-friendly*—if an accident does occur, it is preferable for the turbine to be damaged, so the vessel does not rupture or cause an oil spill[1] (BSH 2015).

In summary, a thorough risk management process can serve two very important purposes—avoiding costly accidents, and demonstrating the safety and reliability of an OWF. This makes good risk management frameworks invaluable to stakeholders from both the maritime and OWF industries.

21.2 Literature Review

When discussing risk management, it is firstly important to define the term *risk* in a theoretical context. Based on a thorough literature review, risk has be defined as *'a combination of the probability and consequences of undesirable events that arise due to a permutation of passive hazards and active failures in a system or a process'* by the current authors.

---

[1]A 160,000 DWT vessel drifting sideways into a turbine at a speed of 2 m/s is often considered as a typical reference case, unless the vessels on a particular route significantly differ in size.

Risk, as a concept, has been widely researched in recent decades. Despite the varying opinions about the actual definition of the term, most authors agree that no system or process is ever risk-free. The risk associated with one system or a process may also have an impact on *other* 'external' systems or processes.

Subsequently, *risk assessment* and *risk management* have emerged as two very vital concepts. *Risk assessment* is an integral part of risk management and refers to the use of tools, methods, models and frameworks to *assess* the risk associated with a system. Once the risk to a system has been assessed, the next step is to evaluate, control and/or monitor the risk; the combination of these latter three steps and the risk assessment process is risk management. The International Risk Governance Council (IRGC) defines risk management as '*the process of analysing, selecting, implementing, and evaluating actions to reduce risk*' (IRGC 2006).

To develop a risk management framework, one must also understand the differences between the three terms *methods, models* and *framework.*

A risk assessment *method* can be thought of as a recipe—it provides step-by-step guidance on assessing the risk associated with a system or a process. A non-exhaustive list of risk assessment methods would include Fault Tree Analyses (FTAs), Event Tree Analyses (ETAs), Risk Contribution Trees (RCTs), Failure mode, effects and criticality analyses (FMEAs/FMECAs), and Bayesian Networks (BNs).

Risk assessment *models*, on the other hand, are replications of real-life systems and processes. Models can be developed using the step-by-step approach provided by a method, although this is not always the case—some simpler models can be developed without the explicit help of a specific method.

A *framework* is an overarching 'outline' which can consist of several methods, models and other tools. A risk *assessment* framework may include guidance as to what should be done before and after the actual risk assessment. For example, a framework may specify what data needs to be collected for an assessment and where/how it can be obtained. Similarly, a risk *management* framework might elaborate on what to do with the results of the risk assessment, and how to interpret them in a meaningful manner, through the use of tools such risk matrices and principles such as ALARP (As Low As Reasonably Practicable). A risk management framework may also contain guidance on the selection and evaluation of different risk control measures, through techniques such as cost-benefit analysis.

Although a detailed review of risk assessment *methods* is out of scope for this book chapter, a review of different risk, probability and consequence assessment *models* and *frameworks* is presented in the following sections.

21.2.1   Maritime Risk Assessment Models for OWFs

Various authors, over the years, have developed maritime risk assessment models for many scenarios—so much so that a complete, exhaustive review is nigh impossible. Review texts range from complete books, to comparison and review

papers (Goerlandt and Montewka 2015; Amdahl et al. 2013; Li et al. 2012; Pedersen 2010; Wang et al. 2002; Soares and Teixeira 2001). It is therefore unfeasible, and redundant, to have a detailed discussion of the various risk assessment models in this report. A brief, categorical overview is, however, prudent.

Risk assessment models can be categorized in many different ways. Some models can be used to calculate the probability of maritime accidents, whilst others focus on the consequences of these accidents. There are models that deal exclusively with a given type of accident, and some models that are applicable to many different types of accidents. For the purpose of this chapter, the author has categorized the risk assessment models based on whether they evaluate the probability, or consequences of accidents. Only models that can be used for maritime risk assessment of maritime operations around offshore wind farms are discussed. The models reviewed cover the risk of contact, collision and grounding events.

21.2.1.1 Probability Models

Geometric – Causation Probability Models for Powered Accidents

A commonly-used method to assess the probability of navigational accidents was proposed by MacDuff (1974). He suggested that the total probability of an accident along a waterway could be expressed as a multiplication of two factors—the 'geometric probability of accident', multiplied by a 'causation probability'. This class of methods is applicable to powered accidents—where a vessel is still under the control of the crew.

Geometric Probability of Accidents

The geometric probability of accidents is simply the probability of an accident occurring if *no evasive measures are taken*. It essentially indicates how often, and how many, vessels deviate from their 'normal' route onto a course that could lead to an accident. Depending on the type of accident, there are many different ways to assess and calculate the geometrical probability of accidents. The most common method is to look at vessel AIS (Automatic Identification System) data for an area, and see how many vessels deviate from their course over a given period of time.

The deviation of the vessels generally depends not only on physical and technical factors related to vessel ways (width of vessel way, marking of objects, aids to navigations, etc.), but also on human factors. A probability distribution of vessel deviations can be created using AIS information, which can be used to assess future case scenarios. Generally, AIS data and probability distributions are enough to calculate the geometric probability of contact (accidents between ships and fixed structures) and grounding accidents (Ellis et al. 2008b; Christensen 2007; Kleissen 2006; ANATEC 2014). AIS data can also be combined with marine spatial data, and information such as bathymetry and geography, to assess the risk of contact or grounding events (Hansen et al. 2013).

The calculation of the geometric probability of accidents can be enhanced by taking into account additional factors—particularly in collision scenarios. For instance, MacDuff (1974) derived a simplified equation to determine the geometric collision candidates based on the manoeuvrability of a vessel, and the width of a channel. Fujii and Tanaka (1971) proposed an equation which took into consideration the traffic density, and the relative speed of colliding vessels. Fujii and Tanaka (1971) also pioneered the concept of a 'collision diameter' or 'ship domain'. A 'collision diameter' is essentially an area enveloping a ship, which—if encroached by another ship—would lead to an imminent collision; this diameter or domain can be calculated using factors such as ship size, manoeuvring capabilities, waterway geometry, and laws of motion (Li et al. 2012).

The concept of a 'collision diameters' and 'ship domains' has been developed further by authors such as Pedersen (2010), Kaneko (2002, 2013) and Montewka et al. (2010b, 2011, 2012)—who have derived their own equations to estimate the number of geometric collision candidates; the latter have developed a concept called 'Minimum Distance to Collision' (MDTC), which incorporates the physical properties of vessels, ship dynamics and even the traffic patterns in an area to assess the risk of ship-ship collisions (Montewka et al. 2012). Equations that incorporate principles of ship domain, in combination with vessel traffic data, are also often used in tools like iWRAP (Friis-Hansen 2008).

Causation Probability of Accidents

The geometric probability, alone, is not enough to assess the probability of an accident; another important value that needs to be assessed is the causation probability. If a vessel is on an accident course, but manages to correct the course in time, the accident can be avoided; thus, the causation probability is essentially the *probability of evasion measures being undertaken* by a vessel on an accident course. When the values of geometric probability and causation probability are combined, one can calculate the *total* probability of a given type of accident.

Causation probabilities are often harder to quantify. MacDuff (1974), Fujii and Yamanouchi (1974), and Fujii et al. (1974) determined causation probabilities through observations, and by considering historical data, to see how often 'incorrect' vessel deviations were corrected before an accident occurred. They came up with specific values of causation probabilities, which are tabulated and still commonly used in modern risk assessment studies and tools—despite the fact that these values were for *specific* maritime areas, from a time long gone. To compensate for this, these outdated causation probability values may be multiplied by a constant factor to provide a conservative estimate, and to reflect the assumption that modern technology has made navigation safer.

Rather than estimating a causation probability based on observations alone, some authors prefer to calculate it instead. Depending on the *type* of accident being analysed, causation probabilities can be calculated in different ways. Calculating causation probability of contact incidents, for example, requires one to take into consideration factors such as the location, and size of a fixed object. Similarly,

to calculate the probability of grounding events, one may have to consider the hydrographic and bathymetric features of a sea area. Causation probabilities equations may be functions of various physical parameters such as vessel speed, vessel type, distance between vessel and accident area/object, and traffic density.

Causation probabilities are also heavily dependent on the so-called 'human element'—i.e.—the capabilities of human beings on board the ship. Human reliability techniques such as HEART (Human error assessment and reduction technique) and THERP (Technique for human error-rate prediction) can be used to quantify the frequency of human error.

Various studies have also quantified the effect of factors such as weather, and bad visibility conditions, on the causation probability (Larsen 1993). Some recent studies of causation probabilities also take into account the effect of technical and technological factors, such as coastal state facilities, VTS, and aids to navigation (Lehn-Schiøler et al. 2013). Technical factors - such as rudder or engine failure - can also influence the causation probability (Hänninen and Kujala 2012).

The socio-technical factors required to estimate causation probabilities may be intrinsically linked. As such, causation probabilities are often calculated through sophisticated risk assessment methods such as Fault Trees, Event Tress (Fowler and Sørgård 2000; Haugen 1991) and Bayesian Networks (Akhtar and Utne 2013; Dai et al. 2013; Hänninen et al. 2013; Hänninen and Kujala 2012; Szwed et al. 2006; Friis-Hansen 2000; Friis-Hansen and Simonsen 2002). Using risk assessment methods can allow various factors—such as human and organizational errors, configuration of the navigational area, navigational aids and markings, bathymetry, and coastal state features such as VTS—to be taken into consideration (Friis-Hansen 2008).

To a certain extent, even the most sophisticated causation probability estimates rely on historical data, and the best way to quantify such data is through the use of accident investigation models—best demonstrated by authors such as Mazaheri et al. (2015b), and Schröder-Hinrichs et al. (2011). Data gathered through accident investigation models can, in turn, be used as an input to risk assessment methods—and thus augment causation probability calculations further.

Other Probability Models for Powered Accidents

The overarching principle to assess the probability of accidents—by combining the geometrical and causation probabilities, as suggested by MacDuff—is still widely used today. There are, however, other ways to assess the probability of accidents in the maritime domain as well.

ANATEC (2014), for example, calculate the probability of collisions by dividing a sea area into a number of cells, and considering the traffic density and number of potential encounters in each cell based on AIS data.

One may also rely *solely* on past accident data to identify a potentially dangerous sea area. A good example for such proactive accident data use can be found in the work of Schröder-Hinrichs et al. (2011); in this study, the authors assessed previous

occurrences of engine room fires to determine what equipment and ship areas were most susceptible to such accidents.

Ohlson (2013) suggests the use of risk assessment methods like FMECA to calculate, amongst other factors, the probability of accidents close to OWFs. Van LU (2012) analysed and compared the usefulness of methods such as FMECA, FTA, ETA, Checklist Method and SWIFT. He also extended his work to cover human reliability methods such as THERP, HEART, ASEP and SPAR-H.

Geijerstam and Svensson (2008) identified several factors that should be taken into consideration when performing a qualitative risk assessment for OWFs; in some cases, such factors, combined with simple expert judgements can be used to qualitatively determine if the chances of accidents are 'high' or 'low', for instance.

Probability Models for Drifting Accidents

Drifting accidents are accidents in which the crew is no longer able to control the vessel—usually due to an engine or steering system/rudder failure. Drifting vessels are more prone to contact and grounding incidents.

Therefore, the first step in calculating the probability of drifting accidents is to calculate the probability of engine or rudder failure, whilst a vessel is in an area where there are other structures or shallow water depths.

One should also take into consideration the sea space available, and the wind and weather conditions in an area—as these factors determine how much a time is available for the vessel to perform corrective action or repairs. If for example, the wind and wave conditions are favourable, and the drift speed is very low, the crew may actually be able to repair the engine or rudder before an accident takes place.

The probability of a vessel anchoring safely before a drifting accident occurs, or being towed to safety by tug vessels, should also be considered. Most modern drifting models and frameworks have specific time functions based on historic ship data, which allow users to assess the time available to a drifting vessel based on all the aforementioned factors (SAFESHIP 2006; Kleissen 2006; van der Tak 2010; Christensen 2007; Ellis et al. 2008b).

21.2.1.2 Consequence Models

Work on modelling the consequences of maritime accidents was pioneered by in the 1950s (Minorsky 1959). Since then, various authors have developed many different consequence assessment models.

As demonstrated by Wang et al. (2002), consequence models can be categorized in many different ways. There are models, for instance, that deal with either internal or external mechanics of ship collisions. Some models take into consideration the deformation of a ship's bow, whilst others may not. Alternatively, models may be classified depending on the type of accident they were developed for—collision, contact or grounding models. Lastly, models can be classified on the *type* of analysis they perform; this is the classification used in this chapter.

Empirical, Analytical, and Probabilistic Consequence Models

Minorsky (1959) proposed to separate the external mechanics and internal mechanics of accidents. External mechanics are generally based on the equations of motions of, and the kinetic energy of the vessel(s) involved. Principles of conservation of energy, momentum and angular momentum (Wang et al. 2002) are generally applied when assessing the external mechanics of ship accidents. Pedersen and Zhang (1998), Zhang (1999), and Pedersen (2014) have done some pioneering work on the external mechanics of ship accidents. Other authors (Simonsen 1997; Paik and Thayamballi 2007) have developed equations for similar approaches.

The internal mechanics study the actual structural and material failure in given accidents. Analysis methods for internal mechanics can be further divided into many sub-categories, based on the type of analysis, and the equations used. Minorsky (1959), for instance developed empirical equations to model the internal mechanics of ship accidents—particularly damage length and penetration—based on past data. Pedersen and Zhang (1998) developed Minorsky's work further, and Zhang (1999) derived semi-empirical, semi-analytical equations for internal mechanics, improving Minorsky's original empirical equations for ship damage.

Pedersen (2002, 2010, 2013, 2014), Pedersen et al. (1993), Zhang (1999), Lützen (2001), Chen (2000), Brown (2001, 2002a, b), Brown and Chen (2002), and Lin (2008), amongst others, have also developed analytical models for analysis of internal mechanics problem.

The analytical models developed by Pedersen (2002, 2010, 2013, 2014) focus mainly on the kinetic energy dissipation, and are based on factors such as mass, speed, and angles and location of collision and contact along the ship length. Brown and Chen (2002) have further developed the programme SIMCOL (Chen 2000; Brown 2002a), which can quickly assess the damage length and penetration depth, with varying parameters such as angle of collision, and speed of ships. Ehlers and Tabri (2012) have developed a robust model to assess the damage to a ship through a semi-analytical, semi-numerical procedure. Tools like GRACAT (Friis-Hansen and Simonsen 2002) have also been developed based on analytical and empirical equations, and can help to assess, and visualize, the damage to ships in an integrated manner—users are able to calculate everything from the probability of collisions and grounding, to the oil outflows and capsizing time.

Aside from considering external and internal mechanics, probabilistic damage assessment is also very common when assessing the consequences of ship accidents. Such models are essentially an offshoot of empirical models, and rely primarily on past accident data. Ronza et al. (2003) and Ellis et al. (2008a) used Event Trees, developed using past-accident data, to predict *likely* future case accidents and consequences. Probabilistic models have been used by the IMO in Formal Safety Assessment studies—not only to predict environmental damage, but also to assess the stability of ships, effectiveness of evacuations and potential loss of lives (IMO 2008). Organizations like ANATEC (2014) also use accident statistics and subsequent predictive estimates to assess the consequences of maritime accidents near OWFs.

Goerlandt and Montewka (2014), amongst others, have developed thorough and robust probabilistic consequence models using methods such as Bayesian Networks, fault trees, and event trees (Li et al. 2012). Similar work has been carried out by Vanem and Skjong (2004), Mazaheri (2009), Montewka (2009), Montewka et al. (2010a, 2014a, b), van de Wiel and van Dorp (2011), Ståhlberg et al. (2013), and Helle et al. (2015), amongst other authors. Some of these aforementioned authors have combined tree-based diagrams with neural networks, and augmented their findings with past accident-data, for further validity.

Finite Element (Numerical) Consequence Models

External and internal mechanics can also be assessed using simplified Finite Element Methods (FEM). Ito et al. (1985) and Paik et al. (1999)—amongst others— have done substantial work in this area. In recent years, with advances in computing, non-linear FEM simulations have become increasingly popular, for the level of detail they are able to capture. Authors like Xia (2001) and Kitamura (2002) have demonstrated the use of FEM for collision and grounding accidents.

Non-linear FEM offers a very robust solution to analyse complex systems like a turbine-vessel collision. Amongst others, Servis and Samuelides (1999) and Xia (2001) have developed FE models for ship-ship collisions, whilst Dalhoff and Biehl (2005), Biehl and Lehmann (2006), Dai et al. (2013), and Bela et al. (2015) have all published papers on FEM for ship-turbine collisions. FEM can also be used to model the damage on the turbine itself, as demonstrated by Ozguc et al. (2006), Le Sourne et al. (2015), Ren and Ou (2009), Ramberg (2011), Kroondijk (2012), Pichler et al. (2012), Samsonovs et al. (2014), Ding et al. (2014), and Hsieh (2015); such models are invaluable as they can incorporate factors such as blade rotation and soil-structure interaction, thus being able to provide an in-depth analysis of contact events. Cho et al. (2013) describe experimental investigations to validate numerical models of OWF collisions.

FE models can provide a comprehensive analysis of internal mechanics—and can thus be used to obtain accurate values for parameters such as damage length, damage height and penetration depth of damage to a ship. This information can then be used to calculate further consequences—e.g.—oil outflow, using models developed by Sirkar et al. (1997), Krata et al. (2012), and Tavakoli et al. (2008, 2010). One can also assess the 'hull girder strength' after an accident to assess the residual strength of a ship; although analytical, empirical and probabilistic equations for doing so are presented by many authors as described by Wang et al. (2002), FE models can provide a more detailed outlook.

Once the extent of damage (damage length, penetration) is known, equations, or software like HECSALV and Seatrack Web can also be used to assess further consequences—economical, environment and social—based on factors such as ship stability, oil outflow/drift, and water-inrush.

Other Consequence Models

As with probability, it is possible to assess consequences of accidents qualitatively. Qualitative models are not commonplace, though they may sometimes be used during the preliminary stages of risk assessment. A qualitative model generally relies on a combination of expert judgements and past data. In his Licentiate, Ohlson (2013) describes a framework where consequences are calculated both quantitatively and qualitatively.

Probability and consequence models are many and varied, and it is safe to say that there is no 'one solution fits all' model. In an ideal framework, it is therefore prudent to select a variety of models that can complement each other and provide a very comprehensive overview of the situation. At the same time, the models should not be too resource intensive, as this would be very unfeasible.

21.2.2 Existing Risk Management Frameworks

From the get-go, thorough risk management of maritime operations OWFs has been considered an important task. Several different industrial organisations have developed integrated frameworks that can assess the risk associated with OWFs. Examples of such frameworks include SAMSON from MARIN (SAFESHIP 2006; Kleissen 2006; van der Tak 2010), CRASH/MARCS from DNV (SAFESHIP 2006; Christensen 2007), and COLLRISK from ANATEC (Ellis et al. 2008b; ANATEC 2014). The existing frameworks are often considered to be robust; they can provide users with very detailed and comprehensive probability calculations and estimates for various types of accidents around OWFs. The frameworks are also able to quantify the consequences in terms of parameters such as damage to property, environmental damage, loss of human lives, etc. to varying degrees of detail and accuracy. Furthermore, these frameworks are very adept at performing cost-benefit analyses of various risk control options.

21.2.2.1 The Gap in Existing Risk Management Frameworks

Despite all their benefits, the existing frameworks have some weaknesses. One concern that stakeholders often have is that the ship damage estimations in these frameworks are very simplistic—often relying on basic kinetic energy calculations, and past accident statistics. This raises doubts as to whether or not these frameworks are sophisticated and detailed enough to adequately assess the consequences of complex accidents, such as vessel-turbine collisions. The lack of adequately detailed consequence assessment may lead to over- or under-designed systems. Moreover, some of these frameworks may be insufficient as approval tools in countries like Germany, which require detailed consequence calculations.

The *transparency* of different frameworks is also a concern previously highlighted by the EU-funded SAFESHIP project and the findings of Ellis et al. (2008b). The latter report implied that it was impossible to replicate the calculation results of certain frameworks, as the equations and data values being used were not evident. Since the study by Ellis et al. (2008b), however, some stakeholders have made greater efforts to increase the transparency and validity of their models and frameworks. Both MARIN and DNV-GL—and even companies like ANATEC— for instance, have produced very clear and detailed reports about their calculation methods. Despite the significant progress in this area by major industry players, some of the frameworks widely used by other organisations and governments still do not conform to an adequate level of transparency. This prevailing lack of transparency does not bode well for a maturing industry.

Ellis et al. (2008b) also highlighted concerns about *harmonisation* of various risk management frameworks. It was noted that despite the initiation of the SAFESHIP project—which was set up to harmonize navigational risk assessment (NRA) models—a harmonized *framework* was not achieved. In their study, Ellis et al. (2008b) compared the risk assessment results for a specific transnational OWF— Krieger's Flak—shared between three different countries: Denmark, Sweden and Germany. It was noted that the NRA had been conducted by different organizations, and that the results of the NRA were quite different for the same wind farm. In fact, each different framework used different tools and models for the calculation of probability and consequences of various undesirable events. This difference in probability and consequence calculations arises because different countries and organizations have different calculation procedures. Going forward, this is clearly as issue that needs to be addressed particularly given the ambitious plans for transnational wind farm.

The lack of harmonization is also a bureaucratic burden as it means that OWF owners have to follow different procedures in different countries. For offshore wind to be viable, such administrative problems should be addressed urgently. The continuing rapid growth of OWFs, increasing sizes and complexity of turbines, and novel developments such as floating turbines (EWEA 2014) further underline the urgent need for harmonization. Thus, harmonizing various risk management frameworks is a high priority task—and one that is advocated by key players in both the maritime and OWF industries; harmonization concerns, for instance, have been highlighted repeatedly by organisations such as the European Wind Energy Association (EWEA 2007).

Lastly, the existing frameworks are often geared towards subject matter experts. This is not a negative *per se*; however, OWFs are complex socio-technical systems, which ideally require various groups of stakeholders from different backgrounds to work together towards an optimal solution. Bearing this in mind, more should be done to involve cross-industry stakeholders in the risk management process.

In summary, existing risk management frameworks have four broadly identifiable gap areas—lack of harmonization, poor transparency, insufficient stakeholder involvement, and inadequately detailed consequence calculations. In order to address these issues, the current chapter describes an improved, unified risk management framework for vessels operating near OWFs.

21.3 The Proposed Risk Management Framework

Based on the problems and research gap identified in the previous sections, a novel theoretical risk management framework has been developed. This framework is designed to provide a step-by-step approach towards harmonized and transparent risk management. Currently, the proposed framework describes the risk management process for vessels *passing* near offshore wind farms only. The authors plan to extend the same framework to include other core maritime risks associated with OWFs, as listed in Sect. 21.1.2.

Some of the steps shown in the following diagrams (Figs. 21.1–21.9) are already incorporated into various existing risk assessment models and frameworks. Therefore, where possible, the authors recommend the relevant tool(s) which can be used to fulfil the respective steps. It is important to note, however, there is no *single* existing model or framework which covers *all* of the steps—this, in fact, is the novelty of the current work.

Even though certain models are *recommended*[2] the current chapter does not provide any specific formulae or detailed explanation (although the reader is provided with appropriate references). This is primarily because the models and tools used have been developed by other authors, and detailed explanations of how the equations are derived are beyond the scope of this chapter. Furthermore, this framework is still *theoretical*—to reiterate, the premise of this chapter is to present the steps that could constitute an improved and unified risk management process. It is therefore intended that any equations will be presented at a future stage.

Figure 21.1 shows the 'main' flowchart of the risk management framework. The boxes in blue indicate the 'pre-risk assessment' or data collection stage. The green boxes are the core of the framework—the 'risk assessment/estimation' stage. The red boxes indicate the 'risk evaluation' and 'risk management' stages—i.e.— stages where decision makers decide if the estimated risk is acceptable, or if further measures are needed to mitigate the maritime risk associated with offshore wind farms.

21.3.1 Pre-risk Assessment (Blue): Steps 1–3

Before beginning any risk assessment, it is vital to collect data that can allow one to calculate the probabilities and consequences of various undesirable events.

The primary data that needs to be collected when performing a risk assessment around an OWF is, of course, data related to the wind farm itself. A project like MARE-WINT has a substantial advantage at this stage, since different researchers try and optimize various different parameters of the OWF. For instance, several

---

[2]The selection of the recommended tools/models is partly based on the input/output capabilities and reasonable resource costs.
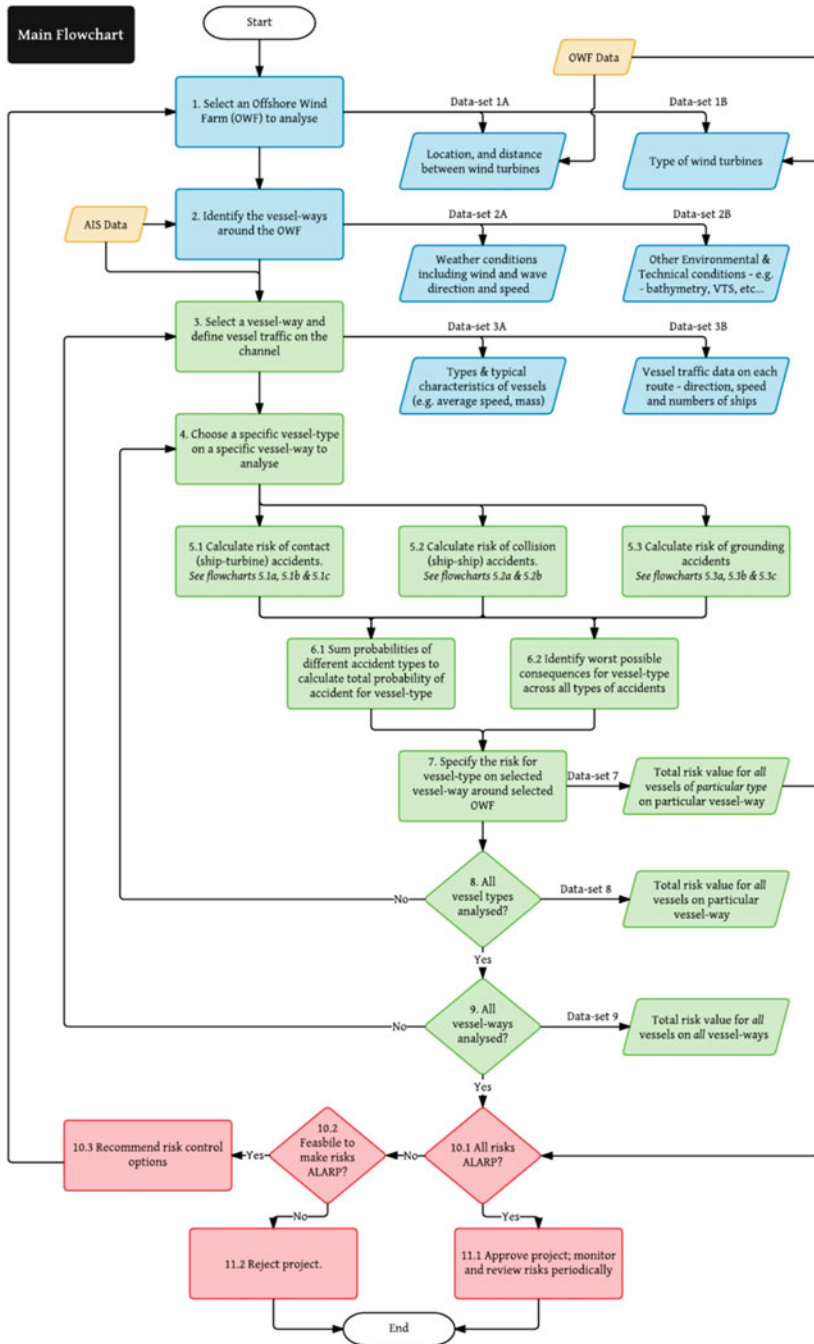
Fig. 21.1 The main/core flowchart for the proposed risk management framework

researchers work directly on the optimization of the support tower and substructure components of a turbine, based on the feedback they receive from other fellows working on blade, gearbox and nacelle design. The work of these researchers is immensely useful for the current research, as it provides structural information about the turbine—which allows one to study the consequences of ship collisions in detail. Similarly, another researcher's work focused on large eddy simulations over the wind farm to optimize the wind farm layout. This work can help to identify the inter-turbine distance, and the proposed layout of the wind farm. The distance between the turbines can affect both the probability, and the consequences of maritime accidents. The output of the proposed framework can also be used to provide feedback *to* other researchers. This iterative approach can improve the design process for OWFs.

Apart from the feedback from other researchers, one of the most important sources of information is Automatic Identification System (AIS) data for vessels. AIS data includes vessel tracks over a given period of time, which can help users to create a statistical distribution of vessel traffic around a potential OWF site.

AIS data also contains other valuable information such as the speed and mass of vessels; it may even be possible to identify manoeuvring characteristics of a vessel, since AIS records the call-signs. AIS data, combined with metrological and hydrography data can allow for a detailed, enhanced risk assessment. All this data is collected and recorded by appropriate marine and maritime agencies, and can be obtained for risk assessment purposes.

21.3.2 Risk Assessment/Estimation (Green): Steps 3–9

The most crucial output from the risk assessment/estimation stage is data-set 7, as shown on Fig. 21.1. This data-set specifies a total risk value for each *type of vessel* on each *vessel way* around a wind farm. Obtaining this value is the core goal for the current framework.

In order to obtain this value, the first step is to define the various vessel ways and the traffic density on each way. This, as stated above, can be done using AIS recordings around the proposed wind farm area. Generally, AIS data recorded over a period of one year just prior to the risk assessment, is considered.

The next step is to define standard parameters for each *type*[3] of vessel that operates on each *vessel way*. This is done in step 4. A 'standard' vessel in this sense would refer to a vessel that is typical of a particular vessel-type. It is proposed that standard vessel data be developed by different member states for risk assessment purposes.

---

[3]Vessels can be classified into different types according to classifications present in literature. Usually, vessels are classified based on their role and the cargo they carry—e.g.—general cargo, bulk, oil tanker, etc . . . This classification is widely used, and is recommended for the proposed framework.

The primary parameters that define the 'standard' vessel include speed, mass, loading condition, and design and construction aspects. The last parameter can be obtained from IMO documents pertaining to minimum design standards; the other factors, such as average speed, can be obtained directly from AIS data, and vessel data over a given period of time. So if, for example, 10 different types of cargo ships operate on one route adjacent to a wind farm, step four would 'average' these 10 cargo ships into one standard cargo ship—which would then be used as a reference in all calculations involving that ship type. This helps to significantly reduce computation and analysis time, particularly if an area with high traffic needs to be assessed. Defining a standard vessel may also allow future case vessels to be taken into consideration. It is also recommended by the author that various coastal states maintain a database of 3D models for 'standard' vessels that can be used during the consequence assessment stage for FE (Finite Element) numerical calculations. These databases can also be regularly updated to accurately reflect the vessels in a given sea area.

Three main types of risks need to be estimated for each type of vessel, as indicated by steps 5.1, 5.2 and 5.3 in Fig. 21.1. The three risks are the risk of contact (an accident involving a vessel and a wind turbine), the risk of a collision (an accident involving 2 or more vessels), and the risk of grounding (an accident where a vessel runs aground). For each type of risk, the user is required to calculate the total probability of that risk, and then determine the worst-case consequences—for each separate type of vessel.

The next few pages contain further flow charts (Figs. 21.2, 21.3, 21.4, 21.5, 21.6, 21.7, 21.8, and 21.9) which explain, step-by-step, how to calculate the probability and consequence values associated with each type of risk. Each time a user goes through the entire *set* of flowcharts, they calculate the risk to all vessels of *one specific type*, on *one specific route* around the OWF. In order to do a complete risk assessment, the users should repeat the process for as many vessel-types as they expect, on as many routes there are around the OWF (steps 8 and 9, Fig. 21.1).

Once a user gets to step 6.1, they should add *all* the probability values for each specific vessel-type. In step 6.2, they should specify *only* the worst case consequences for each specific vessel-type, as quantified in step 5. Combined, these probability and consequence values will give the overall risk associated with all vessels of a particular type, on a particular vessel-way around a wind farm.

21.3.3   Risk of Contact Events: Figs. 21.2, 21.3 and 21.4

The first risk that needs to be calculated is the risk from contact events. Contact events, as stated earlier, involve an accident between a fixed object—in this case, a turbine—and a ship. In order to calculate the overall risk of contact events, a user must first calculate the probability of both powered and drifting contact events individually (Figs. 21.2 and 21.3), and then calculate the consequences (Fig. 21.4).

Flowchart 5.1a

From Step 5.1

Start

5.1.1 Select a point i,j on selected vessel-way

Vessel traffic data on each route - direction, speed and numbers of ships

5.1.2 Calculate geometric probability of contact - i.e. - probability of being at i,j

Location, and distance between wind turbines

5.1.3 At i,j, calculate probability that vessel is heading towards wind farms

Types & typical characteristics of vessels (e.g. average speed, mass)

5.1.4 Calculate probability that vessel will *not* alter course

5.1.5 Calculate probability that vessel will sail into wind farm rather than hitting a turbine

5.1.6 Multiply values 5.1.2 to 5.1.5

Data.set 5.1.6 → Total expected powered contact events for *one* vessel of specific type at *one* specific point

5.1.7 All points on way analysed?

No

Yes

5.1.8 Sum probability of contact at each point i,j for each vessel

Data-set 5.1.8 → Total expected powered contact events for *one* vessel of specific type along *entire* vessel-way

5.1.9 Multiply 5.1.8 by total number of ships of specific vessel-type on vessel-way

Data-set 5.1.9 → Total expected powered contact events for *all* vessels of specific type on *entire* vessel-way

End

To Step 5.1b

Fig. 21.2 Flowchart for step 5.1a: probability of powered contact

Flowchart 5.1b

From Step 5.1a

Start

5.1.10 Calculate probability of engine failure for selected vessel type

Vessel traffic data on each route - direction, speed and numbers of ships

5.1.11 Calculate probability that vessel will drift towards wind farm

Weather conditions including wind and wave direction and speed

Location, and distance between wind turbines

5.1.12 Calculate probability that response measures (anchoring/self-repair/tug) will be unsuccessful in time

Types & typical characteristics of vessels (e.g. average speed, mass)

5.1.13 Calculate probability that vessel will sail into wind farm rather than hitting a turbine

5.1.14 Calculate average time a vessel spends in the area

5.1.15 Multiply values 5.3.10 to 5.3.14

Data.set 5.3.15

Total no. of expected drifting contact events for *one* vessel of specific type along *entire* vessel-way

5.1.16 Multiply 5.1.15 by total number of ships of specific vessel-type on vessel-way

Data-set 5.3.16

Total no. of expected drifting contact events for *all* vessels of specific type on *entire* vessel-way

End

To Step 5.1c

Fig. 21.3 Flow chart for step 5.1b: probability of drifting contact

21.3.3.1 Probability of Powered Contact: Fig. 21.2

A powered contact generally occurs when a vessel is deviating from course and heading towards a wind farm, and this incorrect action is not corrected in time. Therefore, in order to calculate the probability the powered contact, it is recommended that the user follow the geometric-causation probability model as described in Sect. 21.2.1.1.1.
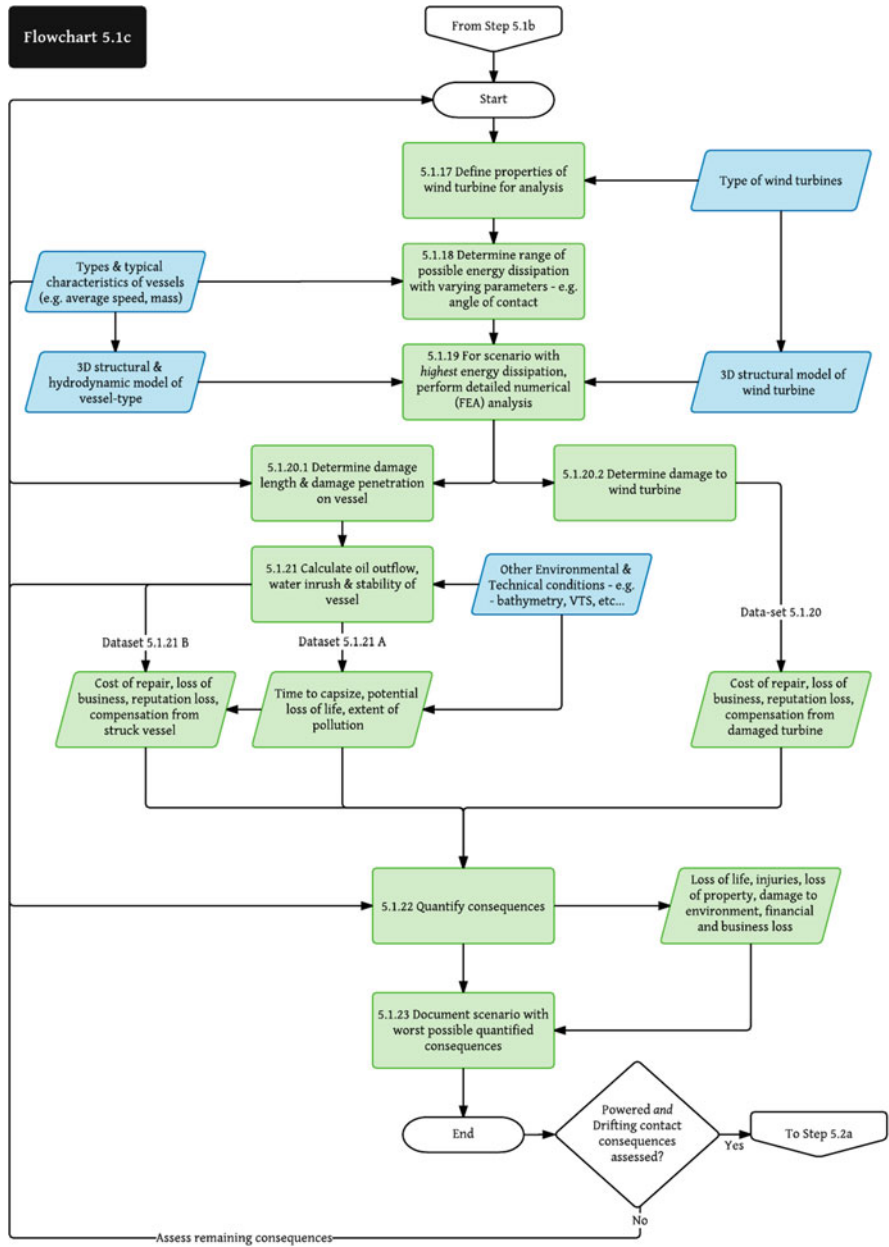
Flowchart 5.1c

From Step 5.1b

Start

5.1.17 Define properties of wind turbine for analysis

Type of wind turbines

Types & typical characteristics of vessels (e.g. average speed, mass)

5.1.18 Determine range of possible energy dissipation with varying parameters - e.g. angle of contact

3D structural & hydrodynamic model of vessel-type

5.1.19 For scenario with *highest* energy dissipation, perform detailed numerical (FEA) analysis

3D structural model of wind turbine

5.1.20.1 Determine damage length & damage penetration on vessel

5.1.20.2 Determine damage to wind turbine

5.1.21 Calculate oil outflow, water inrush & stability of vessel

Other Environmental & Technical conditions - e.g. - bathymetry, VTS, etc...

Data-set 5.1.20

Dataset 5.1.21 B

Dataset 5.1.21 A

Cost of repair, loss of business, reputation loss, compensation from struck vessel

Time to capsize, potential loss of life, extent of pollution

Cost of repair, loss of business, reputation loss, compensation from damaged turbine

Loss of life, injuries, loss of property, damage to environment, financial and business loss

5.1.22 Quantify consequences

5.1.23 Document scenario with worst possible quantified consequences

End

Powered *and* Drifting contact consequences assessed?

To Step 5.2a

Yes

No

Assess remaining consequences

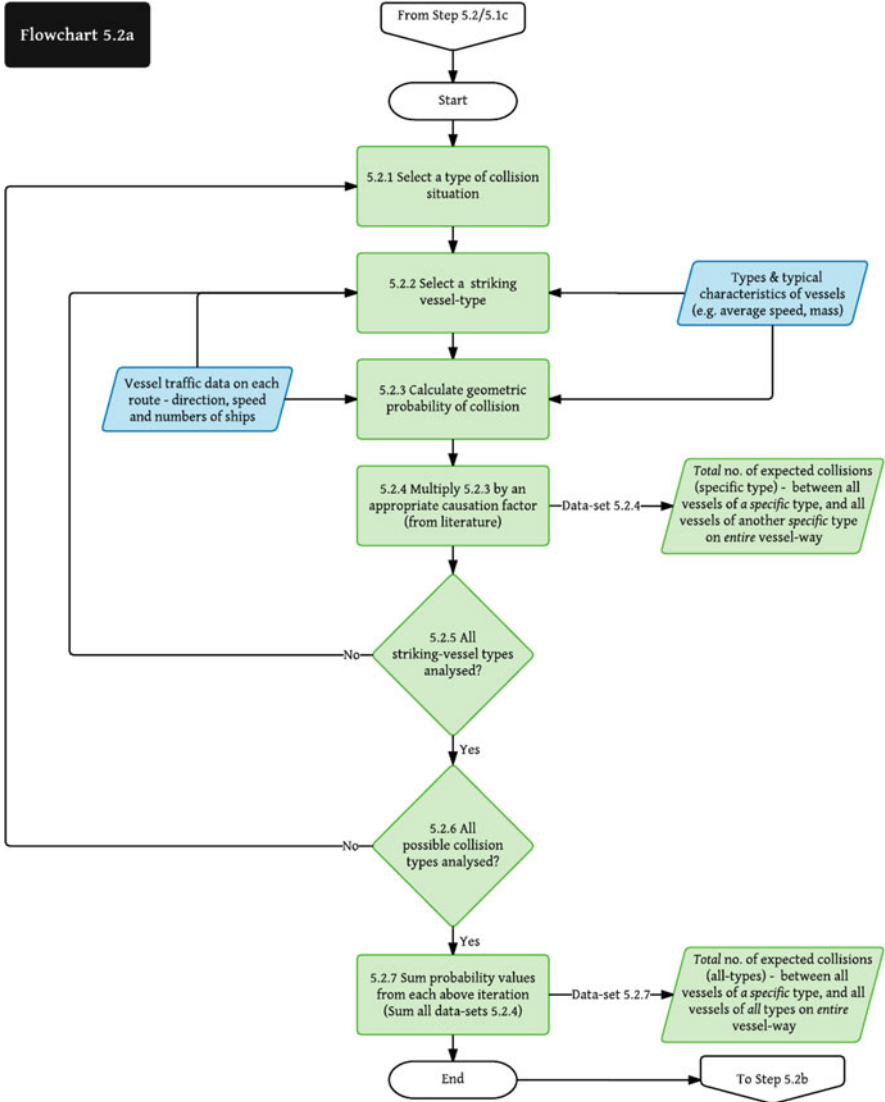**Fig. 21.4** Flowchart for step 5.1c: consequences of contact

Fig. 21.5 Flowchart for step 5.2a: probability of powered collisions

Essentially, a user must first calculate the geometric probability of accident—i.e.—the probability that a vessel is *not* following its course and/or is offset from the vessel way (steps 5.1.2 and 5.1.3 in Fig. 21.2). This is generally done by looking at AIS data, and determining how many times vessels deviate from their route. The AIS data can be used to generate a probability distribution, which indicates how often vessels deviate or are offset from the median line of a vessel way. If AIS data is not available, it is reasonable to assume that vessel traffic is normally distributed along the width of the vessel-way.
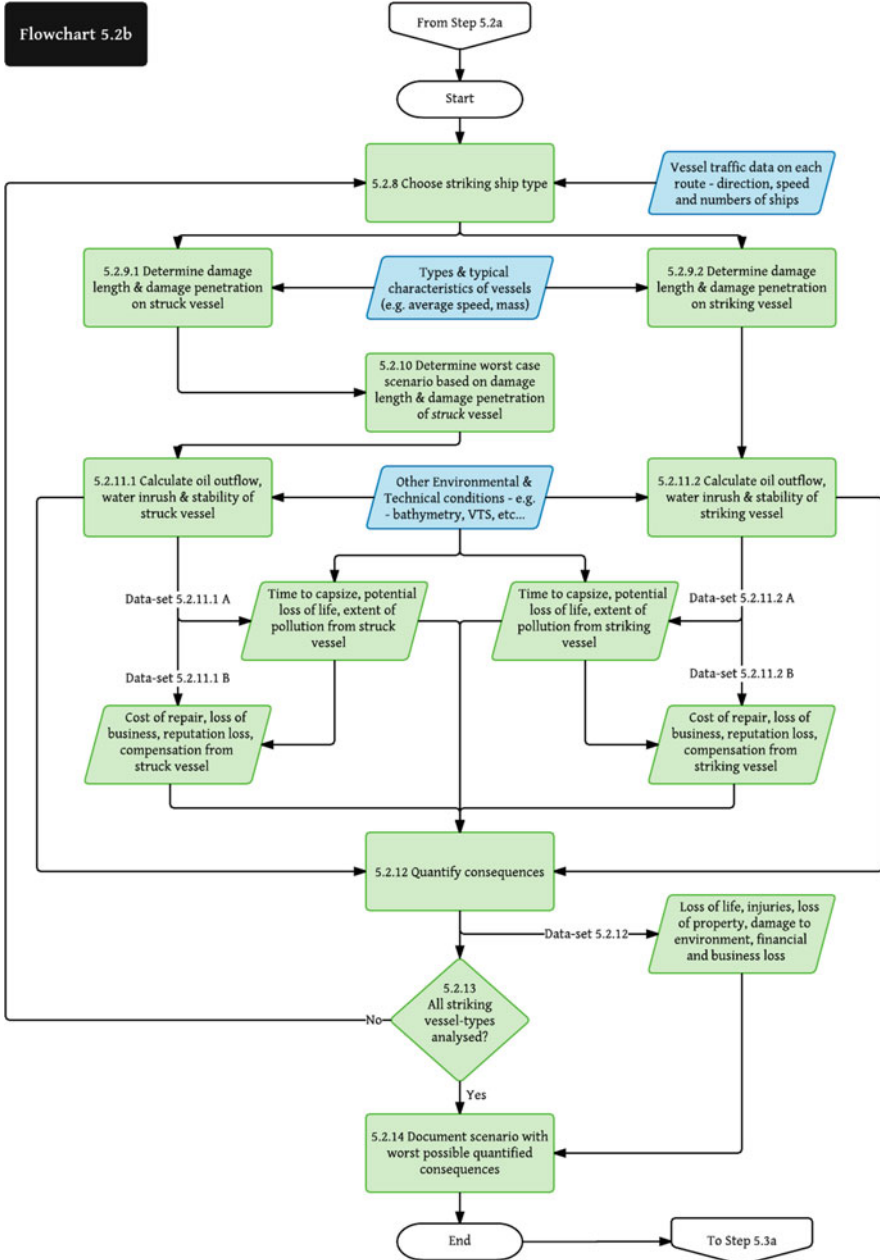
Flowchart 5.2b

From Step 5.2a

Start

5.2.8 Choose striking ship type ← Vessel traffic data on each route - direction, speed and numbers of ships

5.2.9.1 Determine damage length & damage penetration on struck vessel ← Types & typical characteristics of vessels (e.g. average speed, mass) → 5.2.9.2 Determine damage length & damage penetration on striking vessel

5.2.10 Determine worst case scenario based on damage length & damage penetration of *struck* vessel

5.2.11.1 Calculate oil outflow, water inrush & stability of struck vessel ← Other Environmental & Technical conditions - e.g. - bathymetry, VTS, etc... → 5.2.11.2 Calculate oil outflow, water inrush & stability of striking vessel

Data-set 5.2.11.1 A   Time to capsize, potential loss of life, extent of pollution from struck vessel   Time to capsize, potential loss of life, extent of pollution from striking vessel   Data-set 5.2.11.2 A

Data-set 5.2.11.1 B   Cost of repair, loss of business, reputation loss, compensation from struck vessel   Cost of repair, loss of business, reputation loss, compensation from striking vessel   Data-set 5.2.11.2 B

5.2.12 Quantify consequences

Data-set 5.2.12 → Loss of life, injuries, loss of property, damage to environment, financial and business loss

5.2.13 All striking vessel-types analysed? —No

Yes

5.2.14 Document scenario with worst possible quantified consequences

End   To Step 5.3a

Fig. 21.6 Flowchart for step 5.2b: consequences of collisions
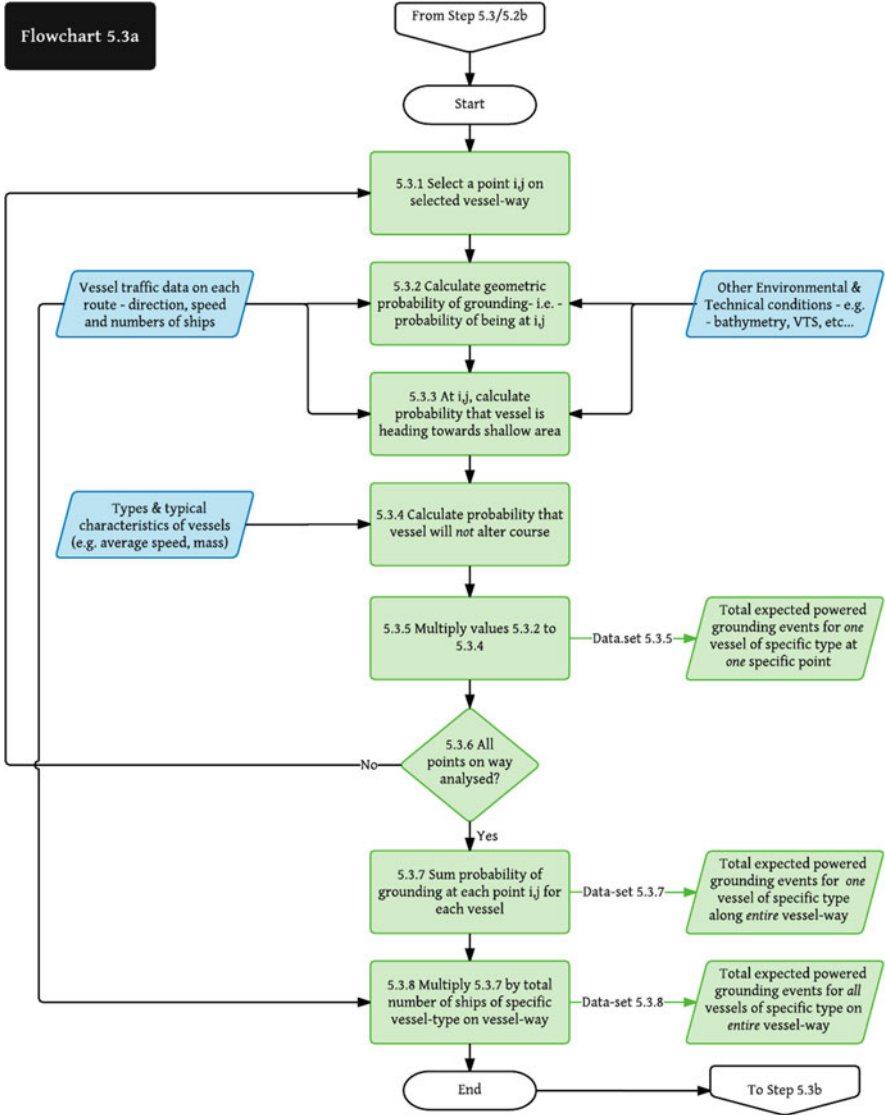
Fig. 21.7 Flowchart for step 5.3a: probability of powered grounding

Calculating the probability of a vessel *not* performing a corrective action, while deviating from its course (step 5.1.4 in Fig. 21.2), is slightly more challenging—particularly because this depends on both human and technical factors. A typical approach is to use a 'causation probability' value from literature; a more sophisticated and thorough approach is use to use risk assessment methods like Fault Trees, Event Trees and Bayesian Networks to estimate the causation probability (Friis-Hansen 2008).
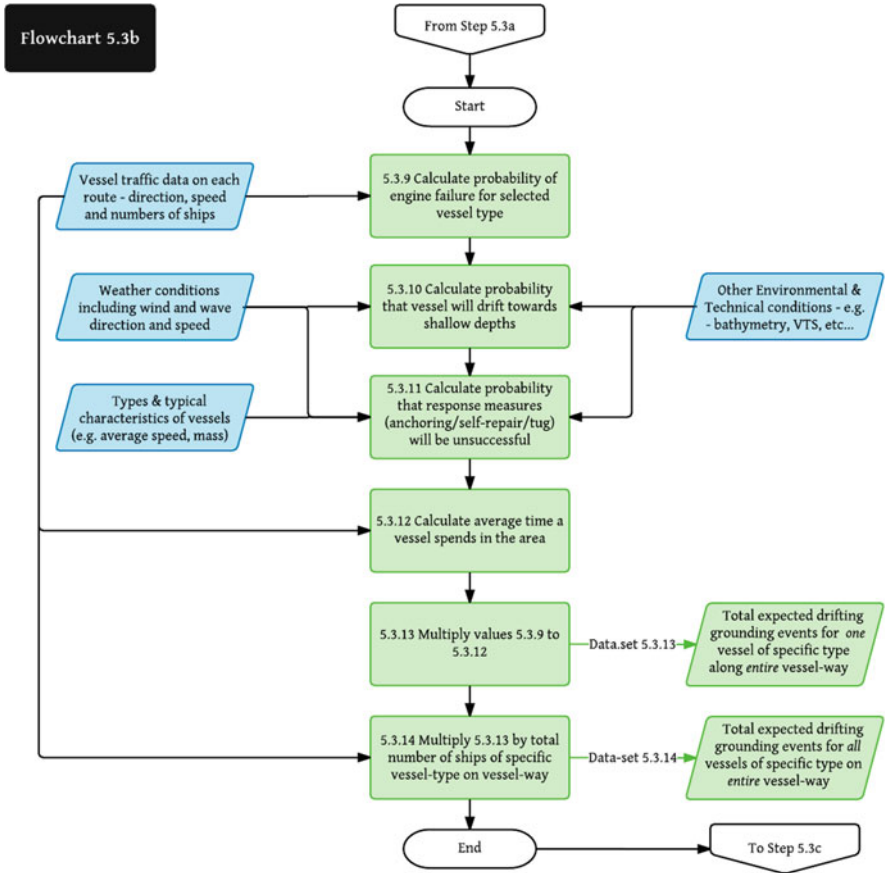
Fig. 21.8 Flowchart for step 5.3b: probability of drifting grounding

Once a user obtains a geometric probability of contact for all vessels over a given time period, and an appropriate causation probability, he or she can then multiply the two values to obtain a total probability of contact for that type of vessel over the given time period.[4]

A user of the framework can also multiply this total probability value by another given geometric equation to calculate the probability of actually hitting a wind turbine rather than just sailing into a wind farm (step 5.1.5 in Fig. 21.2). Equations for this purpose are also available in literature (Ellis et al. 2008b), and generally take into account various factors such as ship length, distance between turbines, and diameters of the turbine towers.

---

[4]The time period that the probability is calculated for is generally 1 year, and therefore the entire traffic over a period of 1 year must be considered (step 5.1.9 in Fig. 21.2).
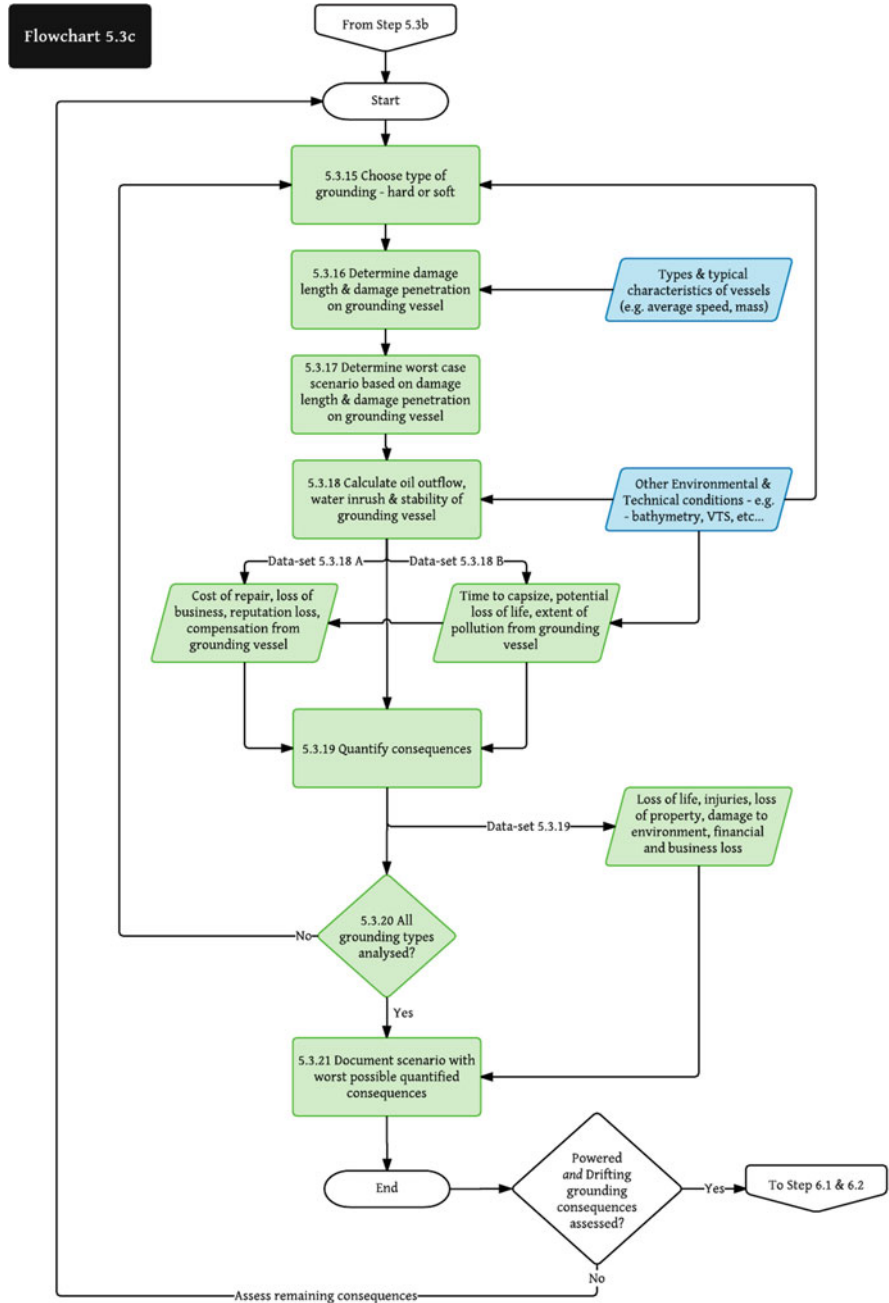
Fig. 21.9 Flowchart for step 5.3c: consequences of grounding

To calculate the probability of a powered contact, the researcher recommends using the model and equations developed by SSPA, as described by Ellis et al. (2008b).

21.3.3.2 Probability of Drifting Contact: Fig. 21.3

Once the probability of powered contact has been calculated, the next step is to calculate the probability of drifting contact (Fig. 21.3). A vessel is set to be 'drifting' when it suffers from loss of engine power. Therefore, in order to calculate the probability of a drifting contact event, a user must first calculate the probability of a vessel-type facing an engine breakdown (5.1.10 in Fig. 21.3). This data is generally available from maritime and ship records.

The next important parameter to calculate during a drifting-contact probability assessment is the probability that a vessel will actually drift *towards* an OWF (5.1.11 in Fig. 21.3). This probability is calculated by looking at wind and wave condition data, and seeing how often the wind or current flows in a direction that can carry ships towards an OWF.

Next, the user must calculate the time for which a vessel will drift—and whether or not this time is enough for a contact accident to occur. In order to do so, the users must consider the width of the traffic distribution on the route, and calculate the time it would take different vessels to reach the wind farm boundary based on their position on the route, and the wind and wave conditions. In the same step, one must also calculate the probability that emergency measures[5] will be unsuccessful or omitted in a given time period (5.1.12 in Fig. 21.3). A successful emergency measure—in time—will ensure that a certain proportion of the vessel traffic will not reach the wind farm to cause a contact incident.

Having obtained all the mentioned parameters, a user can multiply them to calculate the overall probability of a drifting contact for one vessel along an entire vessel way, over a given period of time. Similar to the powered contact procedure, the user can further multiply this product by an equation to obtain the probability of actually drifting and hitting a wind turbine, rather than just drifting into a wind farm area (5.1.13 in Fig. 21.3).

It is also important to predict the potential speed of the vessel in drift. This is vital in order to assess the consequences later. Equations from literature (Kleissen 2006; Christensen 2007; Ellis et al. 2008b) can be used to calculate the drift speed, which depends primarily on current and wind conditions.

For the drifting model, too, the researcher recommends the use of SSPA's comprehensive model and equations, as detailed in Ellis et al. (2008b).

---

[5]Emergency measures generally include anchoring, repairing the ship in time, or getting help from a tug vessel. Each of these measures has a certain probability of success/failure depending on different parameters; typical values for these probabilities are also cited in literature (Ellis et al. 2008b).

To calculate the overall probability of a type of vessel suffering a contact event, a user should sum the probability of both, powered, and drifting contact events for that vessel-type.

21.3.3.3 Consequences of Contact: Fig. 21.4

After calculating the probability of contact, the next step is to calculate the consequences, using Fig. 21.4. To calculate the consequences to a given type of vessel, one should use a 'standard' reference vessel, as explained earlier in this section. A user should also consider the structural properties of a wind turbine (5.1.17 in Fig. 21.4).

The first step (5.1.18 in Fig. 21.4) whilst calculating the consequences is to assess a range of possible energy dissipation values. The energy dissipation values are derived from the range kinetic energy of the vessel when it collides with the turbine, and the energy that the turbine and vessel absorb. Of course, this dissipated energy depends primarily on the velocity and mass of the vessels. Since the speed and mass are assumed to be constant values for all vessels of a specific type, the other parameters that can influence the energy dissipation have to be considered—e.g.— the angle of collision between the ship and the turbine. Therefore, a user must use an equation that relates the mass, velocity *and* the angle of collision, as well as the location of collision, to the kinetic energy. Such equations have been developed by Pedersen and Zhang (1998), and by Pedersen (2002, 2010, 2013, 2014).

Once several kinetic energy values have been obtained, the next step is to perform a detailed numerical finite element analysis (FEA) for the worst case scenario (5.1.19 in Fig. 21.4)—i.e.—the scenario with the highest energy dissipation. Although there are simpler methods to calculate consequences—semi-analytical, probabilistic, and empirical equations being quite common—such methods are geared more towards ship-ship collisions. Without using FEA, it is hard to capture the complexity of a ship-turbine collision, and thus assess the consequences in sufficient detail. A turbine may have many different forces acting upon it, from the aerodynamics of the blades, to the structural integrity of the soil. Therefore, although FEA is more resource intensive, it is the method recommended by the current researcher. Moreover, substantial contemporary literature shows increasing progress when it comes to FEA analysis of ship-turbine contacts. In particular, Biehl and Lehmann (2006) have done significant work on describing numerical methods for ship-turbine collision analysis. Similarly, Dai et al. (2013) describe a procedure to calculate the damage to a turbine, using FEA, in a scenario where a support vessel collides with a wind turbine. Most recently, Bela et al. (2015) have used FEA to assess the crashworthiness of mono-piles.

It is interesting to note that all the above-mentioned papers use the FEA software LS-DYNA for their analysis. In fact, most of the FEA work on ship-turbine collision is done using the software LS-DYNA, as it has certain features (structural element types) which make it ideal for such analysis. Therefore, when it comes to this stage, the current researcher also recommends the use of LS-DYNA. In order to perform

a numerical analysis, the user is required to create a 3D model for each type of vessel, and for each type of wind turbine. The models should incorporate primarily the structural properties, but it is also important to include the hydrodynamic and aerodynamic properties for accurate calculations of consequences. A contact event can then be simulated to assess the energy dissipation in more detail, and to understand the damage to both structures.

A numerical analysis obviously requires a high level of computational resources. The intensity of resources is partially reduced since the FEA is only performed for the worst case scenario for each vessel type, although it is recommended that a user perform it at several different points along the vessel, and at various locations around the turbine to ensure the validity of the results. Developing 3D models and meshing then appropriately consumes a lot of time; in order to minimize this, the author proposes that various coastal states maintain a database of standard meshed 3D models for all vessel types operating in their waters. This can greatly help to reduce the resources required for FE modelling.

A numerical FE analysis allows the user to assess the damage to both the ship and the turbine (5.1.20.1 and 5.1.20.2 in Fig. 21.4). The damage to the wind turbine can determine the state of the turbine after a contact event, and whether it will collapse or not. Such information can be used to evaluate how much economical loss will be incurred.

From the FE calculations, the damage to the ship can be generally visualised, and quantified in terms of a certain damage length, damage height and a specific penetration depth. These parameters in turn define the oil and cargo outflow from a ship, as well as the water inrush. The water inrush can then determine the stability of a ship, and how much time is available until capsize. Using all this information, one can quantify the consequences as described in Fig. 21.4. A similar procedure can be applied to damage incurred by the wind turbine.

For oil outflow, water in rush and stability calculations (5.1.21 in Fig. 21.4), there are equations and models present in literature (van de Wiel and van Dorp 2011; Wang et al. 2002; Li et al. 2012; Goerlandt and Montewka 2014) that can allow a user to model these events; such equations directly relate the extent of damage to the aforementioned parameters. The current researcher, however, uses the software HECSALV from Herbert-ABS to model these events. HECSALV is a rapid assessment tool, developed to perform rapid assessment of vessels in distress. It incorporates widely-used equations to assess several parameters which indicate the state of damage to a vessel. If the damage extent to a ship is known, HECSALV can provide oil outflow estimates, water inrush estimates, and time to capsize estimates, amongst other factors.

The output from HECSALV can be used to estimate evacuation and emergency response times, and, when combined with Data-sets 2A and 2B from Fig. 21.1 (which can indicate the potential level of emergency response in the area), one can estimate the consequences in terms such as loss of lives, amount of total oil spill, and cumulative damage to ship. Methods described by the IMO (2008) can also be used to calculate the potential number of injuries and fatalities. The spreading of oil can be further modelled using tools like Seatrack Web—the official HELCOM oil drift forecasting system.

The consequences of an accident can also be quantified (5.1.22 in Fig. 21.4) as monetary figures, using 'per-unit currency' values given in literature for different types of losses and damages—e.g.—each tonne of oil spill costs approx. $60,000 in a given sea area (Christensen 2007). Such monetary values can be obtained for a variety of consequences—such as loss of one life, loss of a turbine, and damage to environment. Further expert judgements can also be used to augment these monetary values.

Alternatively consequences can be quantified into various qualitative 'levels', although this approach is not recommended for the current framework.

Ideally, the process described by Fig. 21.4 should be repeated twice—once for drifting vessels, and once for powered vessels. The core difference between these two assessments would be speed of the standard colliding vessel—a vessel in drift is likely to have a lower collision speed with a turbine. After quantifying the consequences, it is recommended that *only* the worst-case consequence values be documented for the next stage in the framework—but if the user wishes, they can mention the worst-case consequences for both drifting and powered contact events separately.

21.3.4   Risk of Collision Events: Figs. 21.5 and 21.6

A 'collision' event refers to an accident between 2 or more ships—although the likelihood of there being more than 2 ships is extremely rare. When calculating the risk of collision, it is only necessary to assess the risk of powered collisions. Drifting collisions are extremely unlikely at sea, since it is highly improbable that two vessels will drift towards each other and collide.

21.3.4.1   Probability of Powered Collision: Fig. 21.5

As with powered contact probability, the author recommends using the geometric-causation probability model as described in Sect. 21.2.1.1.1 to calculate the probability of powered collision. Thus, assessing the probability of a powered collision involves the multiplication of two main factors (5.2.4 in Fig. 21.5)—*the geometric collision candidates* and the *causation probability*.

The *causation probability*, as mentioned earlier, is the probability of corrective action being taken; values of causation probability can easily be obtained from various literature sources (Fujii et al. 1974, 1984; Fujii and Mizuki 1998; MacDuff 1974; Ellis et al. 2008b). Alternatively, it can calculated using historical accident data and methods like Bayesian Networks (see Sect. 21.2.1.1.2).

The *number of geometric collision candidates* for collision indicates the likelihood of two vessels occupying the same space, at any given time, if no corrective action is taken. In literature (Pedersen 2010; Li et al. 2012), one can find many equations which provide values for the *geometric collision candidates*, based on the

AIS information for a given area. These equations are different for different types of collision situations; on any given vessel-way, there can be many potential types of collision situations—e.g.—head-on situations, overtaking situations, and crossing situations. It is therefore important, to clearly choose a type of collision situation (step 5.2.1) *before* beginning a collision assessment.

After a user has the values for geometric probability of collision, and appropriate values for causation factors, they can multiply the two values to obtain a *total* probability value. This probability value indicates the frequency of a *given type of collision,* between *all* vessels of *two specific types*, along an *entire* vessel-way, for a *given period of time*. The process should be repeated until all possible collision types and vessel-types have been analysed.

Once the probability of each different *type* of collision has been calculated, the user can sum all these values (step 5.2.7) to get a final probability value: this value would represent the frequency of *all types of collision,* between *one specific vessel type* and *all types of vessels*, along an *entire* vessel-way, for a *given period of time*.

The current researcher recommends using the software tool iWRAP, developed by IALA (Friis-Hansen 2008). iWRAP incorporates all of the steps indicated in Fig. 21.5. It allows users to assess the probability of different *types of* collisions, and can directly assess the geometric collision candidates based on AIS data. iWRAP also has several different causation factors values and ship domain data included, which allows users to perform integrated calculations. The theory and equations behind iWRAP are well-documented, and commonly used by many practitioners. Furthermore, iWRAP is endorsed and recommended by the IMO as an ideal tool to calculate the risk of collision and compare base and future case traffic scenarios—which makes it the perfect tool for the job.

21.3.4.2   Consequences of a Collision: Fig. 21.6

Calculating the consequences for collisions is, in some ways, similar to calculating the consequences of a contact event. One major difference is that the user must select a type of striking ship (5.2.8 in Fig. 21.6), instead of a type of turbine.

Another prime difference is that there is no separate step for energy dissipation calculation. Instead, a range of values for the damage length and damage penetration to each ship are calculated from the very start (5.2.9.1 and 5.2.9.2 in Fig. 21.6). In literature, it is easy to find many equations that relate various parameters—ship speed, mass, loading condition, design, and angle of collision, to name but a few—to damage length and damage penetration in cases of ship-ship collisions (Wang et al. 2002; Pedersen 2010; Li et al. 2012). For the purposes of this framework, the researcher suggests using SIMCOL (Brown 2001, 2002a, b) to assess varying damage lengths and penetration depths with varying factors such as type of striking vessel and angle of collision. SIMCOL uses semi-analytical and empirical equations, which allows for extremely rapid assessment of collision situations with varying parameters.

Once the user has obtained a range of values for damage lengths and penetration depths, he or she should choose the case with the most severe damage to the struck vessel (5.2.10 in Fig. 21.6), to analyse further in terms of oil outflow, stability and water in rush (5.2.11 in Fig. 21.6). Since each type of vessel is analysed based on a standard model, only one case needs to be assessed in detailed. For the chosen case, the consequences can be calculated and quantified in a similar manner to the contact scenario (Sect. 21.3.3.3). It is again recommended to use HECSALV for oil outflow, water in rush and stability calculation, whilst tools like Seatrack Web from HELCOM can be used to model the spread of oil. In other words, 5.2.12 from Fig. 21.6 can be calculated in a similar manner to step 5.1.22 from Fig. 21.4.

Finally, the worst case consequences for each type of vessel, in case of collision events, should then be clearly recorded.

21.3.5 Risk of Grounding Events: Figs. 21.7, 21.8 and 21.9

A grounding event is one where the ship runs into an area of shallow depth, thus causing the bottom of hull to scrape along solid ground, rock or reefs. This type of accident is typically *not* considered when analysing the operation of ships around offshore wind farms. As the number of wind farms increase, however, the limited sea space is reduced. Furthermore, OWFs are often built in shallow waters, and there is a risk of shifting sand banks in some areas. Such factors make an assessment of grounding risk a priority.

21.3.5.1 Probability of Powered Grounding: Fig. 21.7

It is easy to find an abundance of literature on models that calculate the probability of powered groundings (Mazaheri et al. 2014). The current framework recommends a simple approach for this assessment—by suggesting the user to assess the powered grounding probability in a manner similar to the one applied when assessing powered *contact* probability (Fig. 21.2). In fact, between the two approaches (Fig. 21.2 and 21.7), there is only one fundamental difference: when calculating the probability of powered contact, the users have an option to calculate the chance of a ship actually hitting a wind turbine, or just simply sailing into an OWF area; such an option is not available when calculating the powered grounding probability.

To ensure consistency, the researcher recommends the use of iWRAP, which provides a robust calculation procedure for powered grounding. Using iWRAP meets consistency criterion, as it is suggested for collision calculations as well. iWRAP is also able to calculate the probability of grounding for vessel ways with varying geometries and spatial features.

21.3.5.2   Probability of Drifting Grounding: Fig. 21.8

In order to be consistent, the current researcher recommends following a similar procedure to calculate the probability of drifting grounding, as was detailed for assessing the probability of drifting contact events (Fig. 21.3). Once again, the only difference between the process described in Fig. 21.3 and the one described in Fig. 21.8 is that the former allows users to calculate the probability of actually hitting an object, rather than just the probability of drifting into a general area—whereas the latter does not. The researcher again recommends the use of the iWRAP model and/or all its associated equations.

To calculate the overall probability of a type of vessel grounding, a user should sum the probability of powered and drifting grounding events, for that vessel-type.

21.3.5.3   Consequences of Grounding: Fig. 21.9

Many different approaches exist to calculate the consequences of grounding events (Mazaheri et al. 2013, 2014, 2015a, b; Zhu et al. 2002). To assess the consequences of the grounding in a rapid, novel manner, the current frameworks suggests following a similar approach as when assessing the consequences of a collision (Fig. 21.6)—with some differences, of course.

The major difference between the approach outlined in Figs. 21.6 and 21.9 is the exclusion of the 'striking ship' from the latter, and the inclusion of 'grounding type'. Another crucial, but related difference is of course that the consequences are only calculated for one ship at a time, instead of two.

The researcher recommends the use of the same tools and models as used in Fig. 21.6, but with one exception: instead of using SIMCOL to assess the damage length and penetration depth, it is suggested that the procedure outlined by Zhu et al. (2002) is used instead. In this latter procedure, the authors developed equations to allow for a quick assessment of grounding damages (step 5.3.16 in Fig. 21.9), which makes it ideal for use in the current framework.

For the subsequent consequence quantification and assessment, it is once again recommended to use the tools HECSALV and Seatrack Web, along with the per-unit values provided in literature, for various different types of losses.

Ideally, a user should go over Fig. 21.9 twice—once for powered grounding accidents, and once for drifting grounding accidents. The only parameter that will significantly vary between the two cases will be the speed of the grounding. After quantifying the consequences, it is recommended that *only* the worst-case consequence values are documented for subsequent risk evaluation; if the user wishes, however, they can mention the worst-case consequences for both drifting and powered grounding events separately.

21.3.6 Risk Evaluation and Management (Red): Fig. 21.1

21.3.6.1 Risk Evaluation: ALARP and Acceptance Criteria

Having estimated the risk to each type of vessel (steps 5 to 9 in Fig. 21.1), the next steps (10–11) involve *evaluating* the probability and consequence values against certain 'acceptability' criteria. This allows users of the framework to judge whether the risk—to each particular type of vessel along each particular route near the OWF—is acceptably low enough, or not. If a risk to one or more types of vessels is deemed to be too high, the user can implement some risk control measures, and repeat the entire process as described by the framework.

Acceptability criteria are generally set out after consultation with various stakeholders. The International Maritime Organization (IMO) has conducted several studies in which the acceptable criteria for various vessel types are clearly set out (IMO 2006, 2007a, b, 2008). Thus far, however, there have not been any acceptability discussions on vessels specifically operating near OWFs, on an international level.

Despite this, during the planning of OWFs, governments may require the OWF developer to clearly state the acceptable risk. Therefore, companies that carry out navigational risk assessment studies for OWFs occasionally develop acceptability criteria, or matrixes, on a case-by-case basis (ANATEC 2014).

One of the most common ways of checking whether or not a risk is acceptable is through the use of an ALARP diagram (Ellis et al. 2008a). An ALARP diagram is a log-log graph with probability values on the x-axis, and consequence values on the y-axis.

An ALARP diagram can be divided into three sections—*Broadly Acceptable*, *ALARP (As Low as Reasonably Practicable)*, and *Unacceptable.* To demonstrate what an output from the current framework might look like, the author has developed an ALARP diagram using dummy data (Fig. 21.10).

The top right corner, above the white dotted line is the *Unacceptable* region. Risks in this area cannot be accepted by society and/or stakeholders. The region in the bottom left, below the other white dotted line, is the *Broadly Acceptable* region. Ideally, probability and consequence values should be in the region, but it might be unfeasible and costly to design the system for this to be the case. The region in the middle, bounded by the two white dotted lines is the ALARP region. This region indicates the levels of probability and respective consequences are acceptable, and feasible to achieve.[6]

The white ellipses can represent different types of vessels—passing vessels (bulk, general cargo, passenger, RO-PAX, etc.) but also support vessels, SAR vessels

---

[6]The aim of the current framework is to harmonize risk management procedures and *not* the acceptance criteria. Thus, the current framework does not specify limits for the different regions on an ALARP diagram—it is up to the individual maritime administrations and licensing authorities to decide what is 'acceptable' after close consultations with stakeholders.
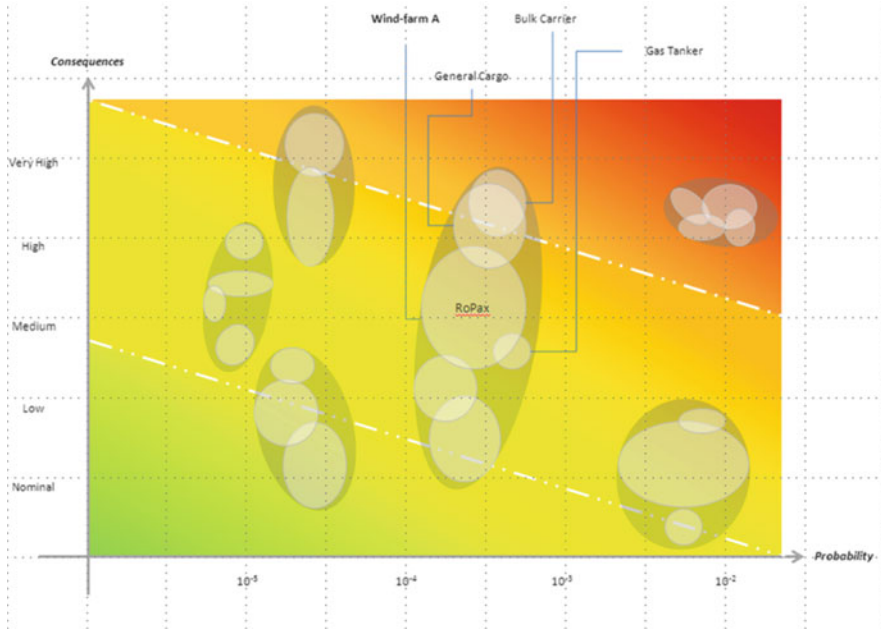
Fig. 21.10 A proposed output of the risk management framework, generated using dummy data

and installation and decommissioning vessels. Each of the grey ellipses indicates different OWF options—various wind turbine layouts, and the effect of various risk control options such as enhanced navigational aids and VTS. The size of the ellipses indicates the uncertainty associated with the calculations; the smaller the size, the more accurate a calculation or estimation is likely to be.

Even if the risk to all vessels is considered to be *acceptable*, it is still important to monitor and review the risks at regular periods over the lifecycle of an OWF. This is particularly important because, over time, some crucial parameters may change; changes may include variations in the standard types of vessels, climate conditions, and technological advances.

21.3.6.2 Risk Management

If a wind farm option lies in the *Unacceptable* region, OWF owners may attempt to mitigate and manage the risk to push it down to the ALARP region. Generally, there are four main ways in which risk can be managed, as identified by various authors and organisations, including the Health and Safety Executive (HSE UK): Risk Avoidance, Retention, Transfer or Reduction and Mitigation.

There is a fundamental difference between risk mitigation and risk avoidance—in the former, the system or process is 'tweaked' to deal with a risk, in the latter the system or process is changed so the risk is eliminated entirely, if possible.

To better understand and summarize the four risk management methods, consider a ship going from point A to B, and passing a wind-farm en-route. The ship therefore faces a possible risk of collision with the wind turbines. If the ship owner wishes to avoid this risk of collision, they might opt for a different route altogether, and thus eliminate a particular risk (although this might give rise to *other* risks). This would be an example of risk avoidance.

Alternatively, the ship owners may decide either that the ship colliding with wind turbines will not harm their interests, or the probability of collision is so low that they are not concerned; they thus decide to do *nothing* about the risk. This option would demonstrate risk retention.

A third option would be to get the ship insured, so that in the case of a collision, the insurance company is responsible for the consequences. This third option exemplifies risk transfer.

Lastly, the ship owner may simply implement some measures that reduce the probability or consequences of collision within the system itself, without eliminating the risk entirely. Such measures could include, for instance, a good captain or state-of-art equipment. This would be an example of risk reduction or mitigation.

To control risk then—primarily via risk avoidance, transfer and mitigation—there are several types of barriers that can be implemented: physical, administrative and supervisory or management barriers. Physical barriers, as the name implies, physically separate the hazard and potential target. Administrative and supervisory and management generally influence, and are influenced by, the human elements in systems and processes. Typically, barriers are designed to either improve the reliability of the system (reduce probability of failures and accidents), or to improve the safety of the system (reduce and mitigate the consequences in case of an accident)—although it is possible to have barriers that reduce *both* the probability and consequences of accidents.

Examples of typical barriers in the maritime domain, that can help to reduce the probability of accidents near OWFs, include measures such VTS (vessel traffic service) monitoring, pilotage, traffic separation schemes, and even sonars (Fricke and Rolfes 2013). There are several consequence-reducing measures as well, proposed by authors such as Graczykowski and Holnicki-Szulc (2009) and Ren and Ou (2009); both their papers describe and analyse the use of 'crashworthiness devices' around the turbine tower, which can minimize the impact of the vessel contact events. The effects of barriers and risk control options can be quantified by going through the process described in the framework (Fig. 21.1), and updating the probability and consequence values for each type of vessel, as necessary. The introduction of VTS, might for example, have an effect on the causation probability of accidents, and this would be reflected in the probability calculations of Fig. 21.1. Similarly, designing an implement to absorb the energy in contact events would mean updated calculations and results for the consequence assessment in Fig. 21.1
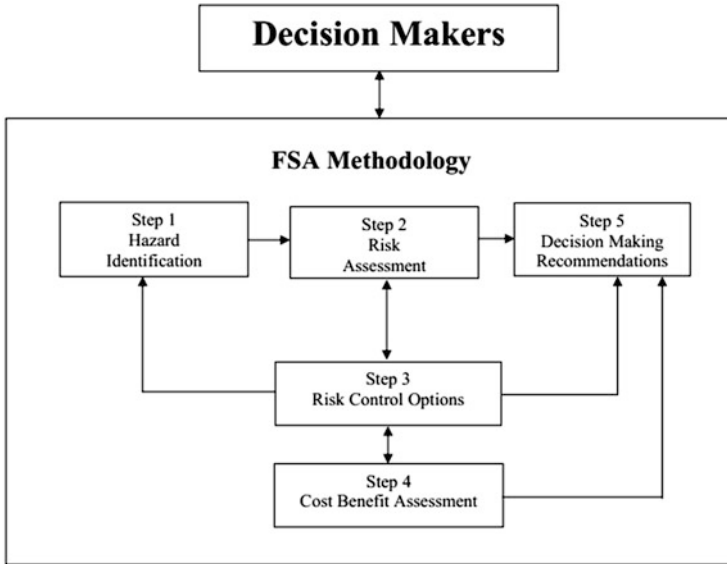
Fig. 21.11 The FSA Process (IMO 2007a)

It is of course, important that risk management measures are feasible, and cost effective. In the maritime domain, the IMO's Formal Safety Assessment (FSA) process was developed for exactly this purpose—to assess the feasibility of risk reduction measures (and new system design). The FSA process consists of 5 steps, as shown in Fig. 21.11.

A detailed breakdown of each of the FSA steps is beyond the scope of this chapter. The risk management framework developed by the researcher attempts to cover all these steps. The risk estimation described by Figs. 21.1, 21.2, 21.3, 21.4, 21.5, 21.6, 21.7, 21.8, and 21.9 cover steps 1 and 2 of the FSA process, whilst the current sub-section deals with steps 3–5. Several IMO documents (IMO 2007a, b, 2008) include specific equations to calculate the 'cost' and 'benefit' of risk reduction measures.

Such analyses are also included in other literature sources such as reports by Christensen (2007) and Kleissen (2006). These equations help decision makers decide if risks associated with a project are worth reducing, or if a project should be abandoned.

21.4   Outlook and Conclusions

With the growing number and sizes of offshore wind farms and turbines, it has become increasingly necessary to conduct proactive risk assessment. Combining the growth of OWFs with developments such as floating wind turbines, and transnational wind farms, one can clearly see that existing frameworks are inadequate. In particular, existing frameworks are not capable of addressing transboundary issues, as risk assessment calculation procedures vary across countries.

This book chapter proposes an urgently-needed harmonized and transparent risk management framework for vessels operating near OWFs. Primarily developed to address the concerns with existing solutions (Sect. 21.2.2.1), the current framework outlines a step-by-step approach, and incorporates various recommended probability and consequence models in a cohesive manner.

Having one uniform framework across several different countries is a big step towards achieving continued growth of OWFs as it can simplify the administrative burdens that developers currently face. A clear, harmonized, step-by-step framework might also encourage smaller OWF owners to submit bids and tenders for OWFs. A simpler, transparent framework may also encourage greater participation from a broader range of stakeholders, thus allowing for a more comprehensive risk assessment. The outputs of this framework can be plotted an ALARP graph (Fig. 21.10)—which can enable quicker, more well-informed decisions from multiple stakeholders.

The proposed framework can, of course, be developed further. One of the immediate next steps will be to define specific equations for each relevant step. The authors also plan to expand this framework to take into account other maritime operations, rather than just vessels *passing* by OWFs. The ALARP diagram for the proposed framework will also be developed further to incorporate a third *cost* axis, which will visualize the results of cost-benefit analysis for various wind farm layouts and risk control options. The proposed framework is, so far, purely theoretical; however, the authors intend to apply this framework to a series of existing and proposed wind farms to validate the work practically in the near future.

Ultimately, the only way that the current levels of OWF growth can be sustained is if both the maritime and OWF industry understand the concerns of the other; the proposed framework is designed to enable just that. To continue building OWFs, we must demonstrate that they are viable, safe and reliable—and the way to do that is through proper, thorough risk management frameworks.

References

Akhtar MJ, Utne IB (2013) Human fatigue's effect on the risk of maritime groundings – A Bayesian Network modelling approach. Saf Sci 62:427–440

Amdahl J, Ehlers S, Leira BJ (eds) (2013) Collision and grounding of ships and offshore structures. CRC Press/Taylor and Francis Group, London

ANATEC, Royal Haskoning DHV (2014) FOREWIND Dogger Bank Teesside A and B – Environmental Statement – Shipping and Navigation (Chapter 16). F-OFL-CH-016 issue 4.1, application reference: 6.16. In: Forewind UK documents. Available via Forewind. http://www.forewind.co.uk/uploads/files/TeessideAB/Application_Documents/6.Environmental_Statement/6.16_ES_Chapter_16_Shipping_and_Navigation.pdf. Accessed 06 Apr 2016

Anderson S (2013) Comparing offshore and onshore wind. In: Harvey Mudd College papers. Available via HMC. http://pages.hmc.edu/evans/andersonwind.pdf. Accessed 06 Apr 2016

Bela A et al (2015) Numerical crashworthiness analysis of an offshore wind turbine monopile impacted by a ship. In: Soares G, Shenoi RA (eds) MARSTRUCT'15. 5th international conference on marine structures, Southampton, March 2015. Analysis and design of marine structures, vol 5. Taylor and Francis Group, London, p 661

Biehl F, Lehmann E (2006) Collisions of ships with offshore wind turbines – calculation and risk evaluation. In: Köller J, Köppel J, Peters W (eds) Offshore wind energy: research on environmental impacts. Springer, Heidelberg, pp 281–304

Brown AJ (2001) Collision scenarios and probabilistic collision damage. In: Pedersen PT, Lützen M, Simonsen BC et al (eds) Proceedings of the 2nd international conference on collision and grounding of ships (ICCGS), Copenhagen, 2001

Brown AJ (2002a) Modelling structural damage in ship collisions. In: Ship structure committee reports. Available via SSC. http://www.shipstructure.org/pdf/422.pdf. Accessed 06 Apr 2016

Brown AJ (2002a) Collision scenarios and probabilistic collision damage. Mar Struct 15:335–364

Brown AJ, Chen D (2002) Probabilistic method for predicting ship collision damage. Ocean Eng 6:54–65

BSH (2015) Minimum requirements concerning the constructive design of offshore structures within the Exclusive Economic Zone (EEZ). In: Federal Maritime and Hydrographic Agency, Germany standards. Available via BSH. http://www.bsh.de/en/Products/Books/Standard/7005-15.pdf. Accessed 06 Apr 2016

Chen D (2000) Simplified ship collision model. Dissertation, Virginia Polytechnic Institute and State University

Cho SR, Seo BS, Cerik BC et al (2013) Experimental and numerical investigations on the collision between offshore wind turbine support structures and service vessels. In: Amdahl J, Ehlers S, Leira BJ (eds) Collision and grounding of ships and offshore structures. CRC Press/Taylor and Francis Group, London, pp 281–288

Christensen CF (2007) Navigational risk assessment – Rødsand 2 wind farm. In: Energy Styrelsen Denmark files. Available via ENS DK. http://www.ens.dk/sites/ens.dk/files/undergrund-forsyning/vedvarende-energi/vindkraft-vindmoeller/havvindmoeller/miljoepaavirkninger/Roedsand/navigational_risk_assessment.pdf. Accessed 06 Apr 2016

Dai L, Ehlers S, Rausand M et al (2013) Risk of collision between service vessels and offshore wind turbines. Reliab Eng Syst Safe 109:18–31

Dalgic Y, Lazakis I, Turan O (2013) Vessel charter rate estimation for offshore wind O&M activities. In: Soares G, Peña FL (eds) Developments in maritime transportation and exploitation of sea resources. CRC Press, Boca Raton, FL, pp 899–907

Dalhoff P, Biehl F (2005) Ship collision, risk analysis – emergency systems – collision dynamics. In: National Renewable Energy Laboratory Documents. Available via NREL. http://wind.nrel.gov/public/SeaCon/Proceedings/Copenhagen.Offshore.Wind.2005/documents/papers/Risk_management/P.Dalhoff_ShipCollision_riskanalysis.pdf. Accessed 06 Apr 2016

Ding H, Zhu Q, Zhang P (2014) Dynamic simulation on collision between ship and offshore wind turbine. Trans Tianjin Univ 20:1–6

Ehlers S, Tabri K (2012) A combined numerical and semi-analytical collision damage assessment procedure. Mar Struct 28:101–119

Ellis J, Forsman B, Gehl S et al (2008a) A risk model for the operation of container vessels. WMU J Marit Aff 7:133–149

Ellis J, Forsman B, Huffmeier J et al (2008b) Methodology for assessing risks to ship traffic from offshore wind farms. In: Vattenfall reports. Available via Vattenfall. https://corporate.vattenfall.se/globalassets/sverige/om-vattenfall/om-oss/var-verksamhet/vindkraft/kriegers-flak/5-kriegers-flak-risk-assessment_11335732.pdf. Accessed 06 Apr 2016

EWEA (2007) Delivering Offshore Wind Power in Europe: Policy recommendations for large-scale deployment of offshore wind power in Europe by 2020. In: The European Wind Energy Association (EWEA) reports and documents. Available via EWEA. http://www.ewea.org/fileadmin/ewea_documents/images/publications/offshore_report/ewea-offshore_report.pdf. Accessed 06 Apr 2016

EWEA (2014) Wind in power: 2013 European statistics. In: The European Wind Energy Association (EWEA) statistics. Available via EWEA. http://www.ewea.org/statistics/. Accessed 06 Apr 2016

EWEA (2015) Wind in power: 2014 European statistics. In: The European Wind Energy Association (EWEA) statistics. Available via EWEA. http://www.ewea.org/statistics/. Accessed 06 Apr 2016

Fowler TG, Sørgård E (2000) Modelling ship transportation risk. Risk Anal 20:225–244

Fricke MB, Rolfes R (2013) Investigation of sonar transponders for offshore wind farms: modeling approach, experimental setup, and results. J Acoust Soc Am 134:3536–3545

Friis-Hansen A (2000) Bayesian networks as a decision support tool in marine applications. Dissertation, Technical University of Denmark

Friis-Hansen P (2008) IWRAP MK II – working document – basic modelling principles for prediction of collision and grounding frequencies. In: IALA-AISM technical products. Available via IALA-AISM. http://www.iala-aism.org/wiki/iwrap/images/2/2b/IWRAP_Theory.pdf. Accessed 06 Apr 2016

Friis-Hansen P, Simonsen BC (2002) GRACAT: software for grounding and collision risk analysis. Mar Struct 15:383–401

Fujii Y, Mizuki N (1998) Design of VTS systems for water with bridges. In: Gluver H, Olsen D (eds) Proceedings of the international symposium on advances in ship collision analysis, Copenhagen, May 1998. Ship collision analysis. A.A. Balkema, Rotterdam, p 177

Fujii Y, Tanaka K (1971) Traffic capacity. J Navig 24:543–552

Fujii Y, Yamanouchi H (1974) Visual range and the degree of risk. J Navig 27:248–252

Fujii Y, Yamanouchi H, Mizuki N (1974) Some factors affecting the frequency of accidents in marine traffic. J Navig 27:239–248

Fujii Y, Yamanouchi H, Matui T (1984) Survey on vessel traffic management systems and brief introduction to marine traffic studies. Electron Navig Res Inst Pap 45:1–48

Geijerstam K, Svensson H (2008) Ship collision risk - an identification and evaluation of important factors in collisions with offshore installations. Dissertation, Lund University

Goerlandt F, Montewka J (2014) A probabilistic model for accidental cargo oil outflow from product tankers in a ship-ship collision. Mar Pollut Bull 79:130–144

Goerlandt F, Montewka J (2015) Maritime transportation risk analysis: review and analysis in light of some foundational issues. Reliab Eng Syst Safe 138:115–134

Graczykowski C, Holnicki-Szulc J (2009) Protecting offshore wind turbines against ship impacts by means of adaptive inflatable structures. Shock Vib 16:335–353

Hänninen M, Kujala P (2012) Influences of variables on ship collision probability in a Bayesian belief network model. Reliab Eng Syst Safe 102:27–40

Hänninen M, Sladojevic M, Tirunagari S et al (2013) Feasibility of collision and grounding data for probabilistic accident modelling. In: Amdahl J, Ehlers S, Leira BJ (eds) Collision and grounding of ships and offshore structures. CRC Press/Taylor and Francis Group, London, pp 1–8

Hansen MG, Randrup-Thomsen S, Askeland T et al (2013) Bridge crossings at Sognefjorden – ship collision risk studies. In: Amdahl J, Ehlers S, Leira BJ (eds) Collision and grounding of ships and offshore structures. CRC Press/Taylor and Francis Group, London, pp 9–18

Haugen S (1991) Probabilistic evaluation of frequency of collision between ships and offshore platforms. Dissertation, University of Trondheim

Helle I, Ahtianen H, Luoma E et al (2015) A probabilistic approach for a cost-benefit analysis of oil spill management under uncertainty – a Bayesian network model for the Gulf of Finland. J Environ Manag 158:122–132

Hsieh JR (2015) Analytical formulations for ship-offshore wind turbine collisions. Dissertation, University of Liege

IMO (2006) Possible improvements on FSA guidelines (MSC 82/INF.3). In: International Maritime Organization (IMO) documents. Available via IMO Docs. https://docs.imo.org/. Accessed 06 Apr 2016

IMO (2007a) Consolidated text of the guidelines for Formal Safety Assessment (FSA) for use in the IMO rule-making process (MSC 83/INF.2). In: International Maritime Organization (IMO) documents. Available via IMO Docs. https://docs.imo.org/. Accessed 06 Apr 2016

IMO (2007b) FSA – Liquefied Natural Gas (LNG) carriers (MSC 83/21/1). In: International Maritime Organization (IMO) documents. Available via IMO Docs. https://docs.imo.org/. Accessed 06 Apr 2016

IMO (2008) FSA – cruise ships – details of the formal safety assessment (MSC 85/INF.2). In: International Maritime Organization (IMO) documents. Available via IMO Docs. https://docs.imo.org/. Accessed 06 Apr 2016

IRGC (2006) Risk governance – towards an integrative approach. In: The International Risk Governance Council (IRGC) publications. Available via IRGC. http://www.irgc.org/IMG/pdf/IRGC_WP_No_1_Risk_Governance__reprinted_version_.pdf. Accessed 06 Apr 2016

Ito H, Kondo K, Yoshimura N et al (1985) A simplified method to analyze the strength of double hulled structures in collision (2nd report). J Soc Nav Archit Jpn 158:420–434

Kaneko F (2002) Methods for probabilistic safety assessment of ships. J Mar Sci Technol 7:1–16

Kaneko F (2013) An improvement on a method for estimating number of collision candidates between ships. In: Amdahl J, Ehlers S, Leira BJ (eds) Collision and grounding of ships and offshore structures. CRC Press/Taylor and Francis Group, London, pp 27–38

Kitamura O (2002) FEM approach to the simulation of collision and grounding damage. Mar Struct 15:403–428

Kleissen F (2006) NSW – MEP: Maritime and marine risk assessment of calamitous (oil) spills. In: NoordzeeWind knowledge, reports and data. Available via Noordzeewind. http://www.noordzeewind.nl/en/knowledge/reportsdata/. Accessed 06 Apr 2016

Krata P, Jachowski J, Montewka J (2012) Modelling of accidental bunker oil spills as a result of ships bunker tanks rupture – a case study. Int J Mar Navig Saf Sea Transp 6(4):495–500

Kroondijk R (2012) High energy ship collisions with bottom supported offshore wind turbines. Dissertation, Norwegian University of Science and Technology

Larsen OD (1993) Ship collision with bridges – the interaction between vessel traffic and bridge structures (structural engineering documents (SED) 4). IABSE-AIPC-IVBH, Zurich

Lehn-Schiøler T, Hansen MG, Melchild K et al (2013) VTS a risk reducer: a quantitative study of the effect of VTS Great Belt. In: Amdahl J, Ehlers S, Leira BJ (eds) Collision and grounding of ships and offshore structures. CRC Press/Taylor and Francis Group, London, pp 19–26

Li S, Meng Q, Qu X (2012) An overview of maritime waterway quantitative risk assessment models. Risk Anal 32:496–512

Le Sourne H, Barrera A, Maliakel JB (2015) Numerical Crashworthiness Analysis of an Offshore Wind Turbine Jacket Impacted by a Ship. J Mar Sci Technol 23(5): 694–704

Lin H (2008) Simplified analysis and design of ships subjected to collision and grounding. Dissertation, Norwegian University of Science and Technology

Lützen M (2001) Ship collision damages. Dissertation, Technical University of Denmark

Macduff T (1974) Probability of vessel collisions. Ocean Ind 9(9):144–148

Mazaheri A (2009) Probabilistic modelling of ship grounding – a review of the literature. In: Kotka Maritime Research Centre publications. Available via Merikotka. http://www.merikotka. fi/safgof/ProbabilisticModelingofShipGrounding.pdf. Accessed 06 Apr 2016

Mazaheri A, Motewka J, Kujala P (2013) Correlation between the ship grounding accidents and the ship traffic – a case study Based on the Statistics of the Gulf of Finland. Int J Mar Navig Saf Sea Transp 7(1):119–124

Mazaheri A, Montewka J, Kujala P (2014) Modelling the risk of ship grounding – a literature review from a risk management perspective. WMU J Marit Aff 13:269–297

Mazaheri A, Montewka J, Kotilainen P et al (2015a) Assessing grounding frequency using ship traffic and waterway complexity. J Navig 68:89–106

Mazaheri A, Montewka J, Nisula J et al (2015b) Usability of accident and incident reports for evidence-based risk modeling – a case study on ship grounding reports. Saf Sci 76:202–214

MCA (2013) Methodology for assessing the marine navigational safety and emergency response risks of offshore renewable energy installations (OREI). In: GOV.UK, Maritime and Coastguard Agency (MCA) documents. Available via GOV.UK MCA. https://www.gov.uk/ government/uploads/system/uploads/attachment_data/file/372597/NRA_Methodology_2013. pdf. Accessed 06 Apr 2016

Minorsky V (1959) An analysis of ship collisions with reference to protection of nuclear power plants. J Ship Res 3:1–4

Montewka J (2009) Predicting risk of collision for oil tankers in the gulf of Finland. J KONBiN 3:17–32

Montewka J, Ehlers S, Tabri K (2010a) Elements of risk analysis for a LNG tanker maneuvering with tug assistance in a harbour. In: Abstracts of the 11th international symposium on practical design of ships and other floating structures COPPE/UFRJ 2010, Rio de Janeiro, 19–24 September 2010

Montewka J, Hinz T, Kujala P et al (2010b) Probability modelling of vessel collisions. Reliab Eng Syst Safe 95:573–589

Montewka J, Goerlandt F, Kujala P (2011) A new definition of a collision zone for a geometrical model for ship-ship collision probability estimation. Int J Mar Navig Saf Sea Transp 5(4):497–504

Montewka J, Goerlandt F, Kujala P (2012) Determination of collision criteria and causation factors appropriate to a model for estimating the probability of maritime accidents. Ocean Eng 40:50–61

Montewka J, Goerlandt F, Kujala P (2014a) On a systematic perspective on risk for formal safety assessment (FSA). Reliab Eng Syst Safe 127:77–85

Montewka J, Ehlers S, Goerlandt F et al (2014b) A framework for risk assessment for maritime transportation systems – a case study for open sea collisions involving RoPax vessels. Reliab Eng Syst Safe 124:142–157

Ohlson J (2013) Broadening horizons – The FMECA-NETEP model, offshore wind farms and the permit application process. Dissertation, Linnaeus University

Ozguc O, Das P K, Barltrop N et al (2006) Numerical modelling of ship collisions based on finite element codes. In: Proceedings of the 3rd international ASRANet Colloqium, Glasgow, 10–12 July 2006

Paik JK, Thayamballi AK (2007) Ship-shaped offshore installations – design, building, and operation. Cambridge University Press, Cambridge

Paik JK, Chung JY, Choe IH et al (1999) On the rational design of double hull tanker structures against collision. In: The Society of Naval Architects and Marine Engineers (SNAME), technical resource library, technical papers. Available via SNAME. http://www.sname.org/pubs/viewtechnicalpaper?DocumentKey=c7798c58-649e-4247-8d96-358e836552ad. Accessed 06 April 2016

Pedersen PT (2002) Collision risk for fixed offshore structures close to high-density shipping lanes. Proc Inst Mech Eng M J Eng Marit Environ 216:29–44

Pedersen PT (2010) Review and application of ship collision and grounding analysis procedures. Mar Struct 2:241–262

Pedersen PT (2013) Ship collisions against wind turbines, quays and bridge piers. In: Amdahl J, Ehlers S, Leira BJ (eds) Collision and grounding of ships and offshore structures. CRC Press/Taylor and Francis Group, London, pp 273–280

Pedersen PT (2014) Risk assessment for ship collisions against offshore structures. In: Soares G, Santos TA (eds) Maritime technology and engineering. CRC Press/Taylor and Francis Group, London, pp 11–24

Pedersen PT, Zhang S (1998) On impact mechanics in ship collisions. Mar Struct 11:429–449

Pedersen PT, Valsgård S, Olsen D et al (1993) Ship impacts: bow collisions. Int J Impact Eng 13:163–187

Pichler T, Pucker T, Hamann T et al (2012) High-performance Abaqus simulations in soil mechanics reloaded – chances and frontiers. In: iMechanica papers. Available via iMechanica. http://imechanica.org/files/Pichler_TUHH_final_2222012.pdf. Accessed 06 Apr 2016

Ramberg HF (2011) High energy ship collisions with bottom supported offshore wind turbines. Dissertation, Norwegian University of Science and Technology

Ren N, Ou J (2009) Dynamic numerical simulation for ship-OWT collision. In: Abstracts of the 8th international conference on reliability, maintainability and safety (ICMRS), Chengdu, 20–24 July 2009

Ronza A, Félez S, Darbra RM et al (2003) Predicting the frequency of accidents in port areas by developing event trees from historical analysis. J Loss Prevent Proc 16(6):551–560

SAFESHIP (2006) Reduction of ship collision risks for offshore wind farms: state of the art of risk models – Deliverable No. 5; Version 1, 2006-10-27, BV, Bunnik

Samsonovs A, Giuliani L, Zania V (2014) Soil structure interaction in offshore wind turbine collisions. In: Cunha A, Caetano E, Ribeiro P et al (eds) Proceedings of the 9th international conference on structural dynamics (EURODYN2014), Porto, 2014

Schröder-Hinrichs JU, Baldauf M, Ghirxi KT (2011) Accident investigation reporting deficiencies related to organizational factors in machinery space fires and explosions. Accid Anal Prev 43(3):1187–1196

Servis DP, Samuelides M (1999) Ship collision analysis using finite elements. In: GL Group research and advanced engineering. Available via GL Research Server. http://research.gl-group.com/Projects/DEXTREMEL/publications/nantes-ntua.pdf. Accessed 06 Apr 2016

Simonsen BC (1997) Mechanics of ship grounding. Dissertation, Technical University of Denmark

Sirkar J, Ameer P, Brown A et al (1997) A framework for assessing the environmental performance of tankers in accidental groundings and collisions. SNAME Trans 105:253–295

Soares CG, Teixeira AP (2001) Risk assessment in maritime transportation. Reliab Eng Syst Saf 74:299–309

Ståhlberg K, Goerlandt F, Ehlers S et al (2013) Impact scenario models for probabilistic risk-based design for ship–ship collision. Mar Struct 33:238–264

Szwed P, van Dorp JR, Merrick JRW et al (2006) A Bayesian paired comparison approach for relative accident probability assessment with covariate information. Eur J Oper Res 169:157–177

Tavakoli MT, Amdahl J, Ashrafian A et al (2008) Analytical predictions of oil spill from grounded cargo tankers; In: Abstracts of the 27th international conference on offshore mechanics and arctic engineering (OMAE'08), Estoril, 15–20 June 2008

Tavakoli MT, Amdahl J, Leira BJ (2010) Analytical and numerical modelling of oil spill from a side damaged tank. In: Ehlers S, Romanoff J (eds) Proceedings of 5th international conference on collision and grounding of ships (ICCGS), Espoo, 2010

Van LU (2012) Risk analysis methods within offshore wind energy. Dissertation, Norwegian University of Science and Technology

van de Wiel G, van Dorp JR (2011) An oil outflow model for tanker collisions and groundings. Ann Oper Res 187(1):279–304

van der Tak C (2010) Quantitative risk assessment for offshore wind farms in the North Sea. Report 23601.621/4. In: Nordzeeloket Netherlands information. Available via Nordzeeloket. https://www.noordzeeloket.nl/images/Quantitative%20risk%20assesment%20for%20offshore %20wind%20farms%20in%20the%20North%20Sea_994.pdf. Accessed 06 Apr 2016

Vanem E, Skjong R (2004) Collision and grounding of passenger ships - risk assessment and emergency evacuations. In: Society of Naval Architects of Japan (ed) Proceedings of 3rd international conference on collision and grounding of ships (ICCGS), Izu, 2004

Wang G, Spencer J, Chen Y (2002) Assessment of a ships performance in accidents. Mar Struct 15:313–333

Xia J (2001) Finite element analysis of ship collisions. Dissertation, Virginia Polytechnic Institute and State University

Zhang S (1999) The mechanics of ship collisions. Dissertation, Technical University of Denmark

Zhu L, James P, Zhang S (2002) Statistics and damage assessment of ship grounding. Mar Struct 15:515–530

Zilakos I, Toulios M, Sameulides M et al (2009) Simulation of the response of double bottoms under grounding actions using finite elements. In: Soares G, Das PK (eds) MARSTRUCT'09. 2nd International conference on marine structures, Lisbon, March 2009. Analysis and design of marine structures. CRC Press/Balkema, Leiden, p 305

Part VII
Offshore Wind Decommissioning